arXiv:cond-mat/0312286v1 11 Dec 2003

Radiative corrections to the excitonic molecule state in GaAs microcavities

A. L. Ivanov
Department of Physics and Astronomy, Cardiff University,
Queen's Buildings, Cardiff CF24 3YB, United Kingdom

P. Borri, W. Langbein, and U. Woggon
Lehrstuhl für Experimentelle Physik EIIb, Universität Dortmund, Otto-Hahn Str.4, 44227 Dortmund, Germany

(Dated: February 2, 2008)

The optical properties of excitonic molecules (XXs) in GaAs-based quantum well microcavities (MCs) are studied, both theoretically and experimentally. We show that the radiative corrections to the XX state, the Lamb shift $\Delta_{\rm XX}^{\rm MC}$ and radiative width $\Gamma_{\rm XX}^{\rm MC}$, are large, about $10-30\,\%$ of the molecule binding energy $\epsilon_{\rm XX}$, and definitely cannot be neglected. The optics of excitonic molecules is dominated by the in-plane resonant dissociation of the molecules into outgoing 1λ-mode and 0λ-mode cavity polaritons. The later decay channel, "excitonic molecule $\rightarrow$ 0λ-mode polariton + 0λ-mode polariton", deals with the short-wavelength MC polaritons invisible in standard optical experiments, i.e., refers to "hidden" optics of microcavities. By using transient four-wave mixing and pump-probe spectroscopies, we infer that the radiative width, associated with excitonic molecules of the binding energy $\epsilon_{\rm XX} \simeq 0.9-1.1\,$meV, is $\Gamma_{\rm XX}^{\rm MC} \simeq 0.2-0.3\,$meV in the microcavities and $\Gamma_{\rm XX}^{\rm QW} \simeq 0.1\,$meV in a reference GaAs single quantum well (QW). We show that for our high-quality quasi-two-dimensional nanostructures the $T_2 = 2T_1$ limit, relevant to the XX states, holds at temperatures below $10\,$K, and that the bipolariton model of excitonic molecules explains quantitatively and self-consistently the measured XX radiative widths. A nearly factor two difference between $\Gamma_{\rm XX}^{\rm MC}$ and $\Gamma_{\rm XX}^{\rm QW}$ is attributed to a larger number of the XX optical decay channels in microcavities in comparison with those in single QWs. We also find and characterize two critical points in the dependence of the radiative corrections against the microcavity detuning, and propose to use the critical points for high-precision measurements of the molecule binding energy and microcavity Rabi splitting.

PACS numbers: 78.66.-w,78.47.+p,78.66.Fd,71.36.+c

I. INTRODUCTION

The optical properties of an excitonic molecule originate from the resonant interaction of its constituent excitons (Xs) with the light field. For semiconductor (GaAs) nanostructures we analyze in this paper, the above interaction refers to quasi-two-dimensional (quasi-2D) QW excitons and is different in single, MC-free quantum wells and in microcavities. In the first case, the breaking of translational invariance along the growth direction (z-direction) leads to the coupling of QW excitons to a continuum of bulk photon modes. This results in an irreversible radiative decay of low-energy QW excitons into the bulk photon modes and to interface, or QW, polaritons for the QW exciton states lying outside the photon cone[1,2,3]. An interface polariton is the in-plane propagating eigenwave guided by a single QW, and the light field associated with interface polaritons is evanescent, i.e., it decays exponentially in the z-direction. In contrast, the MC polariton optics deals with the quasi-stationary mixed states of quasi-2D MC photons and QW excitons[4,5], i.e., one realizes a nearly pure 2D exciton-photon system with resonant coupling between two eigenmodes (for a review of the MC polariton optics see, e.g., Refs. [6,7]). In this case the radiative lifetime of MC polaritons originates from a finite transmission through the cavity mirrors. The main aim of the present work is to develop coherent optics of quasi-2D excitonic molecules in semiconductor microcavities.

The XX-mediated optical response from GaAs microcavities has been addressed only recently[8,9,10,11,12,13,14]. The Coulombic attractive interaction of cross-circular polarized (σ^+ and σ^-) excitons, which gives rise to the XX bound state, has been invoked and estimated in order to analyze the frequency-degenerate four-wave mixing (FWM) experiment[8]. Pump-probe specroscopy was used in Ref. [9] to observe the XX-mediated pump-induced changes in the MC reflectivity spectrum. However, in the above first experiments the microcavity polariton resonance has large broadening so that the spectrally–resolved XX transition was not detected. Only recently the spectrally–resolved "polariton $\leftrightarrow$ XX" photon-assisted transition in GaAs-based MCs has been observed by using differential reflection spectroscopy[10,11]. In particular, the transition is revealed in a pump–probe experiment as an induced absorption from the lower polariton dispersion branch to the XX state, at positive pump-probe time delays[10]. In the latter work the MC Rabi splitting $\Omega_{1\lambda}^{\rm MC}$, associated with a heavy–hole QW exciton, exceeds the XX binding energy $\epsilon_{\rm XX}$ for more than a factor of three. The last experiments on excitonic molecules in GaAs microcavities use a high-intensity laser field to investigate the XX-mediated changes in the polariton spectrum[12,13] and parametric scattering of MC polaritons[14]. In this work we are dealing with a *low-intensity* limit of the XX optics, aiming to study the radiative corrections to the molecule state in a high-quality GaAs single QW embedded in a co-planar λ-cavity. Recently, the optical properties of large binding energy excitonic molecules in a MC-embedded ZnSe QW has been studied[15]. The theoretical model we work out can straightforwardly be adapted to the quasi-2D molecules in II-VI nanostructures.

In the previous theoretical studies[16,17] the XX radiative corrections are not included, so that the models deal with the optically unperturbed molecule wavefunction $\Psi_{\rm XX}$ and binding energy $\epsilon_{\rm XX}$. According to Ref. [16], the XX radiative corrections are rather small, even if $\Omega^{\rm MC}_{1\lambda} \gg \epsilon_{\rm XX}$. The authors argue qualitatively that a volume of phase space, where the resonant coupling of the constituent excitons with the light field occurs, is rather small to affect the XX state. As we show below, an exactly-solvable bipolariton model[18,19], adapted to excitonic molecules in GaAs-based quasi-2D nanostructures, yields $\Gamma^{\rm MC}_{\rm XX}$ and $\Delta^{\rm MC}_{\rm XX}$ of about $(0.15-0.30)\,\epsilon_{\rm XX}$ for microcavities, and $\Gamma^{\rm QW}_{\rm XX}$ and $\Delta^{\rm QW}_{\rm XX}$ of about $(0.10-0.15)\,\epsilon_{\rm XX}$ for single QWs. The calculated values refer to the weak confinement of QW excitons and QW excitonic molecules we deal with in our study. In the weak confinement limit, the QW thickness d_z is comparable with the in-plane radius of the above electron-hole bound complexes, which are still constructed in terms of well-defined transversly-quantized quasi-2D electronic states. In contrast, in the strong confinement limit, d_z is much less than the in-plane radius of QW excitons (excitonic molecules).

The radiative corrections to the XX state cannot be neglected, because the exciton-photon coupling (polariton effect) changes the dispersion of excitons not only in a very close vicinity of the resonant crossover between the relevant exciton and photon energies, but in a rather broad band $p \sim p_0$. Here wavevector p_0 is given by the resonant condition $\hbar\omega^{\gamma}(p_0) = cp/\sqrt{\varepsilon_b} = E_{\rm X}(p_0)$ between the bulk photon and exciton dispersions (ε_b is the background dielectric constant). For GaAs structures $p_0 \simeq 2.7\times10^5\,{\rm cm}^{-1}$. The dimensionless parameter $\delta^{\rm (D)}_{\rm R}$, which scales the XX radiative corrections, is $\delta^{\rm (D)}_{\rm R} = (a^{\rm (D)}_{\rm XX}p_0)^{\rm D}$, where $a^{\rm (D)}_{\rm XX}$ is the molecule radius and D is the dimensionality of a semiconductor structure. Remarkably, as we demonstrate below, $\delta^{\rm (2D)}_{\rm R}$ does not depend upon the MC detuning between the λ-cavity mode and $E_{\rm X}$, i.e., is the same for microcavities and single QWs. For our high-quality GaAs QWs with weak confinement of excitons one estimates $a^{\rm (2D)}_{\rm XX} \simeq 200\,\mathring{A}$, so that $\delta^{\rm (2D)}_{\rm R} \simeq 0.3$. The latter value clearly shows that the exciton-photon coupling does change considerably the quasi-2D XX states. Even for the X wavevectors far away from the resonant crossover point p_0, the polariton effect can still have a considerable impact on the dispersion of optically-dressed excitons in bulk semiconductors and QWs. To illustrate this, note that for bulk GaAs, e.g., the effective mass associated with the upper polariton dispersion branch at $p=0$ is given by $M_{\rm eff} \simeq M_x/4$, i.e., by factor four is less than the translational mass M_x of optically undressed excitons. In a similar way, the dispersion of QW excitons dressed by MC photons, which gives rise to $\Delta^{\rm MC}_{\rm XX}$ and $\Gamma^{\rm MC}_{\rm XX}$, refers to the in-plane wavevector domain $p_{\|} \lesssim p_0$ rather than to a close vicinity of the crossover point $p_{\|} \simeq 0$.

An excitonic molecule can be described in terms of two quasi-bound polaritons (bipolariton), if the coupling of the molecule with the light field is much stronger than the incoherent scattering processes. In this case the sequence "two incoming polaritons (or bulk photons) → quasi-bound XX state → two outgoing polaritons" is a completely coherent process of the resonant polariton-polariton scattering and can be described in terms of the bipolariton wavefunction $\tilde{\Psi}_{\rm XX}$. The latter includes an inherent contribution from the outgoing (incoming) polaritons and should be found from the bipolariton wave equation. The solution also yields the radiative corrections to the XX energy, i.e., $-\epsilon_{\rm XX} = -\epsilon^{(0)}_{\rm XX} + \Delta_{\rm XX} - i\Gamma_{\rm XX}/2$, where $\epsilon^{(0)}_{\rm XX}$ is the "input" XX binding energy of an optically inactive molecule. For some particular model potentials of σ^+-exciton – σ^--exciton interaction, e.g., for the deuteron and Gaussian potentials, the bipolariton wave equation can be solved exactly[18,19]. The bipolariton concept was verified in high-precision experiments with low-temperature bulk CuCl[20,21,22] and CdS[23], and was also applied successfully to explain the XX-mediated optical response from GaAs/AlGaAs multiple QWs[24]. The latter experiment dealt with quasi-2D XXs in the limit of strong QW confinement. In this case the bipolariton model shows that the main channel of the optical decay of QW excitonic molecules in MC-free structures is the resonant photon-assisted dissociation of the molecule into two outgoing interface (QW) polaritons. Note that the Coulombic interaction between two constituent excitons of the molecule couples the radiative modes and the interface polariton states, so that an "umklapp" process between the modes can intrinsically be realized. The above picture refers to the following scenario of the coherent optical generation and dissociation of QW molecules: "σ^+ bulk photon + σ^- bulk photon → σ^+ virtual QW exciton + σ^- virtual QW exciton → QW molecule → σ^+ interface polariton + σ^- interface polariton".

The experiments we report on deal with weakly confined QW excitonic molecules, i.e., the QW thickness $d_z = 250\,\mathring{A}$ is comparable with the radius of excitons in bulk GaAs. The quasi-2D weak confinement allows us to neglect inhomogeneous broadening in the detected X- and XX-mediated signals. The MC-free single QW is used as a reference structure: All the λ-microcavities, which we study, are embedded with a single QW nearly identical to the reference one. By analyzing the coherent dynamics of the XX-mediated signal in spectrally-resolved transient FWM, we infer the XX radiative width in the microcavities and in the reference single QW, $\Gamma^{\rm MC}_{\rm XX}$ and $\Gamma^{\rm QW}_{\rm XX}$, respectively. The measurements yield $\Gamma^{\rm MC}_{\rm XX}$ larger than $\Gamma^{\rm QW}_{\rm XX}$ by nearly factor two. Furthermore, by using pump-probe spectroscopy we also estimate the XX binding energies $\epsilon^{\rm MC}_{\rm XX}$ and $\epsilon^{\rm QW}_{\rm XX}$. Our measurements deal with the MC detuning band $-2\,{\rm meV} \lesssim \delta \lesssim +2\,{\rm meV}$.

Similarly to quasi-2D XXs in high-quality single QWs, the main mechanism of the optical decay of MC molecules is their in-plane resonant dissociation into MC polaritons. Thus the coherent optical path of the XX-mediated signal in our experiments is given by "σ^+ (pump) bulk photon + σ^- (pump) bulk photon → MC molecule → σ^+ MC polariton + σ^- MC polariton → σ^+ (signal) bulk photon + σ^- (signal) bulk photon". The latter escape of the MC polaritons into the bulk photon modes is due to a finite radiative lifetime of MC photons. In order to explain the experimental data, the bipolariton model is adapted to weakly confined quasi-2D molecules in (GaAs) microcavities and MC-free (GaAs) single QWs. One of the most important features of the optics of excitonic molecules in microcavities is a large contribution to the bipolariton state $\tilde{\Psi}_{\mathrm{XX}}$ from 0λ-mode MC polaritons. The relevant 0λ-mode polariton states refer to the in-plane wavevectors $p_\| \sim p_0$, i.e., are short-wavelength in comparison with the 1λ-mode polariton states activated in standard optical experiments. An "invisible" decay channel of the MC molecule into two outgoing 0λ-mode polaritons in combination with the directly observable dissociation path "XX → 1λ-mode MC polariton + 1λ-mode MC polariton" explain qualitatively the factor two difference between $\Gamma^{\mathrm{MC}}_{\mathrm{XX}}$ and $\Gamma^{\mathrm{QW}}_{\mathrm{XX}}$. The use of the microcavities embedded with a single QW allows us to apply the bipolariton model without complications due to the dark X states in multiple QWs[16]. The bipolariton model quantitatively reproduces our experimental data and predicts new spectral features, like $M_{1,2}$ critical points in the detuning dependent $\Gamma^{\mathrm{MC}}_{\mathrm{XX}} = \Gamma^{\mathrm{MC}}_{\mathrm{XX}}(\delta)$ and $\Delta^{\mathrm{MC}}_{\mathrm{XX}} = \Delta^{\mathrm{MC}}_{\mathrm{XX}}(\delta)$.

Thus the main results of our study on weakly confined quasi-2D molecules in GaAs microcavities are (i) rigorous justification of the bipolariton model, (ii) importance of the XX radiative corrections, and (iii) existence of the efficient "hidden" XX decay channel, associated with 0λ-mode MC polaritons.

In Sec. II, we apply the bipolariton model in order to analyze the XX radiative corrections, the XX Lamb shift Δ_{XX} and XX radiative width Γ_{XX}, relevant to our microcavities and reference QW. After a brief discussion of interface and MC polaritons, we demonstrated that in GaAs-based quasi-2D structures the XX radiative corrections can be as large as $10-30\,\%$ of the (input) XX binding energy $\epsilon^{(0)}_{\mathrm{XX}}$. It is shown that independently of the MC detuning δ the XX radiative corrections in microcavities and (reference) QWs are scaled by the same dimensionless parameter $\delta^{(\mathrm{2D})}_{\mathrm{R}} = (a^{(\mathrm{2D})}_{\mathrm{XX}} p_0)^2$, and that the main XX optical decay channels in microcavities are "XX → 1λ-mode MC polariton + 1λ-mode MC polariton" and "XX → 0λ-mode MC polariton + 0λ-mode MC polariton" against the main decay path in single QWs, "XX → interface polariton + interface polariton". We also find and classify two *critical points*, M_1 and M_2, in the spectrum of the XX radiative corrections in microcavities, $\Gamma^{\mathrm{MC}}_{\mathrm{XX}} = \Gamma^{\mathrm{MC}}_{\mathrm{XX}}(\delta)$ and/or $\Delta^{\mathrm{MC}}_{\mathrm{XX}} = \Delta^{\mathrm{MC}}_{\mathrm{XX}}(\delta)$, and propose to use the critical points for high-precision measurements of the MC Rabi splitting and the XX binding energy.

In Sec. III, the investigated GaAs-based MC sample and the reference GaAs single QW are characterized. We describe the FWM measurements at $T = 9\,\mathrm{K}$, which allow us to estimate the XX dephasing width for the MC detuning band $-2\,\mathrm{meV} \lesssim \delta \lesssim 2\,\mathrm{meV}$, $\tilde{\Gamma}^{\mathrm{MC}}_{\mathrm{XX}}(T = 9\,\mathrm{K}) \simeq 0.3-0.4\,\mathrm{meV}$, and the pump-probe experiments at $T = 5\,\mathrm{K}$, which yield the bipolariton (XX) binding energy in our microcavities, $\epsilon^{\mathrm{MC}}_{\mathrm{XX}} \simeq 0.9-1.1\,\mathrm{meV}$.

In Sec. IV, by analyzing a temperature-dependent contribution to the dephasing widths $\tilde{\Gamma}^{\mathrm{MC}}_{\mathrm{XX}}$ and $\tilde{\Gamma}^{\mathrm{QW}}_{\mathrm{XX}}$, which is associated with XX – LA-phonon scattering, we estimate the corresponding XX radiative widths in the microcavities and reference QW ($\Gamma^{\mathrm{MC}}_{\mathrm{XX}} \simeq 0.2-0.3\,\mathrm{meV}$ and $\Gamma^{\mathrm{QW}}_{\mathrm{XX}} \simeq 0.1\,\mathrm{meV}$), and show that the bipolariton model does reproduce *quantitatively and self-consistently* both $\Gamma^{\mathrm{MC}}_{\mathrm{XX}}$ and $\Gamma^{\mathrm{QW}}_{\mathrm{XX}}$. It is shown that the $T_2 = 2T_1$ limit, which is crucial for the validity of the bipolariton model, starts to hold for excitonic molecules at cryostat temperatures below 10 K. We also discuss the underlaying physical picture responsible for the large XX radiative corrections in high-quality quasi-2D (GaAs) nanostructures.

A short summary of the results is given in Sec. V.

II. THE BIPOLARITON STATES IN MICROCAVITIES AND SINGLE QUANTUM WELLS

In this Section we briefly discuss interface (quantum well) and microcavity polaritons, and apply the bipolariton model[18,19] in order to calculate the XX radiative corrections and to describe the optical decay channels of excitonic molecules in high-quality GaAs-based microcavities and single QWs.

A. Interface and microcavity polaritons

For a single QW, the resonant coupling of excitons with the light field can be interpreted in terms of the radiative in-plane modes $|\mathbf{p}_\|| \leq p_0$, which ensure communication of low-energy QW excitons with incoming and outgoing bulk photons (the only photons used in standard pump-probe optical experiments with QWs), and interface polaritons, which refer to the states outside the photon cone, $|\mathbf{p}_\|| \geq \omega_t \sqrt{\varepsilon_b}/c$. The latter in-plane propagating polariton eigenmodes are trapped and waveguided by the X resonance; they are accompanied by the evanescent, interface light field, i.e., are invisible at macroscopic distances from the QW.

For an ideal QW microcavity the MC photons with in-plane wavevector $\mathbf{p}_\|$ can be classified in terms of $n\lambda$-transverse eigenmodes ($n = 0, 1, 2, ...$). The MC polariton eigenstates arise when some of the MC photon eigenmodes resonate with the QW exciton state. As we show below, only 0λ- and 1λ- polariton eigenmodes are relevant to the optics of QW excitonic molecules in our MC structures. With increasing MC thickness towards infinity the microcavity polariton eigenstates evolve into the radiative and interface polariton eigenmodes associated with a MC-free single QW[5].

(i) *The light field resonantly interacting with quasi-2D excitons in a single (GaAs) QW.* The interaction of a QW exciton with in-plane momentum $\hbar \mathbf{p}_\parallel$ with the transverse light field of frequency ω is characterized by the dispersion equation[1,2,3]:

$$\frac{c^2 p_\parallel^2}{\varepsilon_b} = \omega^2 + \frac{\omega^2 R_{\mathrm{X}}^{\mathrm{QW}} \sqrt{p_\parallel^2 - \varepsilon_b(\omega/c)^2}}{\omega_t^2 + \hbar\omega_t p_\parallel^2/M_x - i\omega\gamma_{\mathrm{X}} - \omega^2} \; , \qquad (1)$$

where M_x is the in-plane translational X mass, $\hbar\omega_t = E_{\mathrm{X}}(\mathbf{p}_\parallel{=}0)$ is the X energy, γ_{X} is the rate of incoherent scattering of QW excitons, and $R_{\mathrm{X}}^{\mathrm{QW}}$ is the dimensional oscillator strength of exciton-photon interaction per QW unit area. Equation (1) refers to a single (GaAs) QW confined by two identical (AlGaAs) bulk barriers.

For $|\mathbf{p}_\parallel| \geq \omega\sqrt{\varepsilon_b}/c$, i.e., for the momentum-frequency domain outside the photon cone, Eq. (1) describes the in-plane polarized transverse interface polaritons (Y-mode polaritons). The evanescent light field associated with the interface polaritons is given by $\mathbf{E}(\omega, \mathbf{p}_\parallel, z) = \mathbf{E}(\omega, \mathbf{p}_\parallel)\exp(-\kappa|z|)$, where $\kappa = \sqrt{p_\parallel^2 - \varepsilon_b(\omega/c)^2}$. The exciton and photon components of a QW polariton with in-plane wavevector $\mathbf{p}_\parallel$ are

$$u_{\mathrm{IP}}^2(p_\parallel) = \frac{\kappa R_{\mathrm{X}}^{\mathrm{QW}}}{\kappa R_{\mathrm{X}}^{\mathrm{QW}} + 2[\omega_t + \hbar p_\parallel^2/2M_x - \omega_{\mathrm{IP}}(p_\parallel)]^2} \; ,$$
$$v_{\mathrm{IP}}^2(p_\parallel) = 1 - u_{\mathrm{IP}}^2(p_\parallel) \; , \qquad (2)$$

respectively. Here $\omega = \omega_{\mathrm{IP}}(p_\parallel)$ is the polariton dispersion determined by Eq. (1). Note that the z-polarized transverse interface polaritons (Z-mode QW polaritons) associated with the ground-state heavy-hole excitons are not allowed in GaAs QWs[3].

The low-energy QW excitons from the radiative zone $|\mathbf{p}_\parallel| \leq p_0 = \omega_t\sqrt{\varepsilon_b}/c$ couple with bulk photons, i.e., can radiatively decay into the bulk photon modes. In this case Eq. (1) yields the X radiative decay rate into bulk in-plane (Y-) polarized transverse photons:

$$\frac{1}{\hbar}\Gamma_{\mathrm{X}}^{\mathrm{QW}}(p_\parallel) = \frac{\varepsilon_b}{c^2} R_{\mathrm{X}}^{\mathrm{QW}} \frac{\omega_t}{\sqrt{p_0^2 - p_\parallel^2}} \; . \qquad (3)$$

One can also re-write Eq. (3) as $\Gamma_{\mathrm{X}}^{\mathrm{QW}}(p_\parallel) = \Gamma_{\mathrm{X}}^{\mathrm{QW}}(p_\parallel{=}0)\, p_0/(p_0^2 {-} p_\parallel^2)^{1/2}$, where $\Gamma_{\mathrm{X}}^{\mathrm{QW}}(p_\parallel{=}0) = \hbar(\sqrt{\varepsilon_b}/c)R_{\mathrm{X}}^{\mathrm{QW}}$ is the radiative width of a QW exciton with in-plane momentum $\hbar p_\parallel = 0$. In high-quality GaAs QWs at low temperatures, the condition $\Gamma_{\mathrm{X}}^{\mathrm{QW}} \gg \hbar\gamma_{\mathrm{X}}$ can be achieved, so that the X dispersion within the photon cone is approximated by $\hbar\omega_{\mathrm{X}}^{\mathrm{QW}}(p_\parallel{\leq}p_0) = \hbar\omega_t + \hbar^2 p_\parallel^2/2M_x - i\Gamma_{\mathrm{X}}^{\mathrm{QW}}(p_\parallel)/2$.

The oscillator strength $R_{\mathrm{X}}^{\mathrm{QW}}$ associated with QW excitons is given by

$$R_{\mathrm{X}}^{\mathrm{QW}} = \frac{4\pi}{\hbar}\,\frac{\omega_t}{\varepsilon_b}\,|\phi_{\mathrm{X}}^{(2\mathrm{D})}(\mathbf{r}=0)|^2\,|d_{\mathrm{cv}}|^2 \, , \qquad (4)$$

where $\phi_{\mathrm{X}}^{(2\mathrm{D})}(r)$ is the X wavefunction of relative electron-hole motion, and d_{cv} is the dipole matrix element of the interband optical transition. In the limits of strong and weak QW confinement Eq. (4) yields

$$R_{\mathrm{X}}^{\mathrm{QW}} = \begin{cases} 16 a_{\mathrm{X}}^{(3\mathrm{D})}\omega_{\ell t}\omega_t \, , & a_{\mathrm{X}}^{(3\mathrm{D})} \gg d_z \, , \\ 2 d_z \omega_{\ell t}\omega_t \, , & \lambda = 2\pi/p_0 \gg d_z \gtrsim a_{\mathrm{X}}^{(3\mathrm{D})} \, , \end{cases} \qquad (5)$$

respectively, where $a_{\mathrm{X}}^{(3\mathrm{D})}$ is the Bohr radius of bulk excitons and $\omega_{\ell t}$ is the longitudinal-transverse splitting associated with bulk excitons (in bulk GaAs one has $a_{\mathrm{X}}^{(3\mathrm{D})} \simeq 136\,\text{\AA}$ and $\hbar\omega_{\ell t} \simeq 80 - 86\,\mu$eV, respectively[25]). Thus we estimate the upper limit of the oscillator strength in narrow GaAs QWs as $\hbar^2 R_{\mathrm{X}}^{\mathrm{QW}}(d_z{\to}0) \simeq 0.26 - 0.28\,\mathrm{eV}^2\text{\AA}$. For our GaAs QWs with weak confinement of excitons one evaluates from Eq. (5) that $\hbar^2 R_{\mathrm{X}}^{\mathrm{QW}}(d_z{=}250\,\text{\AA}) \simeq 0.061\,\mathrm{eV}^2\text{\AA}$.

(ii) *The MC polariton dispersion relevant to excitonic molecules in (GaAs-based) microcavities.* The dispersion equation for MC polaritons, which contribute to the XX-mediated optics of a λ-cavity we study in our experiments, is given by

$$\omega_t^2 \; + \; \hbar\omega_t p_\parallel^2/M_x - i\omega\gamma_{\mathrm{X}} - \omega^2 =$$
$$= \; \omega^2 \left[\frac{(\Omega_{1\lambda}^{\mathrm{MC}})^2}{(\omega_{1\lambda}^{\gamma})^2 - i\omega\gamma_{\mathrm{R}} - \omega^2} \; + \; \frac{(\Omega_{0\lambda}^{\mathrm{MC}})^2}{(\omega_{0\lambda}^{\gamma})^2 - i\omega\gamma_{\mathrm{R}} - \omega^2} \right] , \qquad (6)$$

where the photon frequencies, associated with the 1λ- and 0λ- microcavity eigenmodes, are $\omega_{1\lambda}^{\gamma} = \omega_{1\lambda}^{\gamma}(p_\parallel) = (c^2 p_\parallel^2/\varepsilon_b + \omega_0^2)^{1/2}$ and $\omega_{0\lambda}^{\gamma} = \omega_{0\lambda}^{\gamma}(p_\parallel) = cp_\parallel/\sqrt{\varepsilon_b}$, respectively. Here $\omega_0 = (2\pi c)/(L_z\sqrt{\varepsilon_b})$ is the cavity eigenfrequency, L_z is the MC thickness, and γ_{R} is the inverse radiative lifetime of MC photons, due to their escape from the microcavity into external bulk photon modes. The MC Rabi frequency $\Omega_{1\lambda}^{\mathrm{MC}}$ refers to 1λ-eigenmode of the light field, $\hat{\mathrm{e}}_{1\lambda}(z) = \sqrt{2/L_z}\cos[(2\pi z)/L_z]$ (we assume that the QW is located at $z = 0$ so that $|z| \leq L_z/2$), and is determined by

$$(\Omega_{1\lambda}^{\mathrm{MC}})^2 = \frac{16\pi}{\hbar}\,\frac{\omega_t}{\varepsilon_b}\,|\phi_{\mathrm{X}}^{(2\mathrm{D})}(\mathbf{r}=0)|^2\,|d_{\mathrm{cv}}|^2\,\frac{|I_1|^2}{L_z} \, , \qquad (7)$$

where $I_1 = I_1(d_z/L_z) = [L_z/(\pi d_z)]\sin[(\pi d_z)/L_z] \simeq 1 - (\pi/6)(d_z/L_z)^2$. In turn, the Rabi frequency $\Omega_{0\lambda}^{\mathrm{MC}}$ is associated with 0λ-eigenmode of the MC light field, $\hat{\mathrm{e}}_{0\lambda}(z) = 1/\sqrt{L_z} = \mathrm{const.}$, and

$$(\Omega_{0\lambda}^{\mathrm{MC}})^2 = \frac{8\pi}{\hbar}\,\frac{\omega_t}{\varepsilon_b}\,|\phi_{\mathrm{X}}^{(2\mathrm{D})}(\mathbf{r}=0)|^2\,|d_{\mathrm{cv}}|^2\,\frac{1}{L_z} \, . \qquad (8)$$

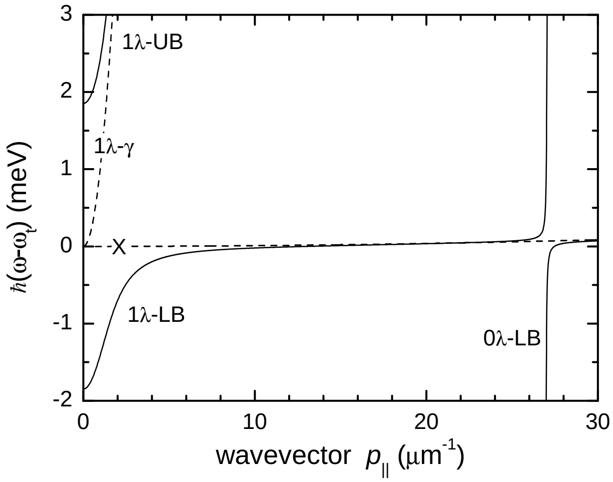

FIG. 1: Three-branch microcavity polariton dispersion calculated with Eq. (6) for zero-detuning. The parameters are adapted to the GaAs microcavities used in our experiments: $\hbar\Omega^{\rm MC}_{1\lambda} = 3.70\,$meV, $\hbar\Omega^{\rm MC}_{0\lambda} = 2.67\,$meV, $\varepsilon_b = 12.3$, $M_x = 0.4\,m_0$, and $E_{\rm X}(p_{\|}{=}0) = \hbar\omega_t = 1.5219\,$eV. The dashed lines show the 1λ-mode MC photon and exciton dispersions (the 0λ-mode photon dispersion is not plotted).

From Eqs. (4), (7), and (8) one gets

$$(\Omega^{\rm MC}_{1\lambda})^2 = 2|I_1|^2(\Omega^{\rm MC}_{0\lambda})^2 = 4\,\frac{R^{\rm MC}_{\rm X}}{L_z}\,|I_1|^2\,. \qquad (9)$$

Because the factor $|I_1|^2 \simeq 1$ (for our microcavities $d_z = 250\,\mathring{A}$ and $L_z \simeq 2326\,\mathring{A}$, so that $|I_1|^2 \simeq 0.96$), we conclude that $\Omega^{\rm MC}_{1\lambda} \simeq \sqrt{2}\Omega^{\rm MC}_{0\lambda} \simeq 2(R^{\rm MC}_{\rm X}/L_z)^{1/2}$. The factor two difference between $(\Omega^{\rm MC}_{1\lambda})^2$ and $(\Omega^{\rm MC}_{0\lambda})^2$ originates from the difference of the intensities of the light fields associated with microcavity 1λ- and 0λ-eigenmodes at the QW position, $z = 0$, i.e., is due to $|\hat{\rm e}_{1\lambda}(z{=}0)|^2/|\hat{\rm e}_{0\lambda}(z{=}0)|^2 = 2$.

Thus, the dispersion Eq. (6) deals with a *three-branch* MC polariton model. In Fig. 1 we plot the polariton dispersion branches, designated by 1λ-UB (upper branch), 1λ-LB (middle branch), and 0λ-LB (lower branch), respectively, and calculated by Eq. (6) for a zero-detuning GaAs-based microcavity with $\hbar\Omega^{\rm MC}_{1\lambda} = 3.70\,$meV and $\hbar\Omega^{\rm MC}_{0\lambda} = 2.67\,$meV. The ratio between the Rabi frequencies satisfies Eq. (9), and the used value of $\Omega^{\rm MC}_{1\lambda}$ corresponds to that observed in our experiments. For small in-plane wavevectors $|\mathbf{p}_{\|}| \lesssim p^{(1\lambda)}_{\|} \simeq 0.5\times10^5\,\rm cm^{-1}$ (see Fig. 1) the 1λ-UB and 1λ-LB dispersion curves are identical to the upper and lower MC polariton branches calculated within the standard 1λ-eigenmode resonant approximation[6,7]. In this case the 1λ-UB and 1λ-LB polaritons are purely 1λ-eigenwaves; the 0λ-LB dispersion is well-separated from the X resonance so that in Eq. (6) one can put $\Omega^{\rm MC}_{0\lambda} = 0$ in order to describe the 1λ-UB and 1λ-LB dispersions in the wavevector domain $p_{\|} \lesssim p^{(1\lambda)}_{\|}$. The anti-crossing between the X dispersion $\omega_t + \hbar p_{\|}^2/2M_x$ and the MC 0λ-mode photon frequency $cp_{\|}/\sqrt{\varepsilon_b}$, which occurs at $p_{\|} = p_0 \simeq 2.7\times10^5\,\rm cm^{-1}$, gives rise to the MC 0λ-eigenmode dispersion associated with the 1λ-LB and 0λ-LB short-wavelength polaritons with $p_{\|} \gg p^{(1\lambda)}_{\|}$ (see Fig. 1). This picture is akin to the two-branch polariton dispersion in bulk semiconductors; for $p_{\|} \simeq p_0$ the 1λ-LB and 0λ-LB polariton dispersion can accurately be approximated by Eq. (6) with $\Omega^{\rm MC}_{1\lambda} = 0$. In this case Eq. (6) becomes identical to the dispersion equation for bulk polaritons, if in the latter the bulk Rabi splitting $\Omega^{\rm bulk}$ ($\hbar\Omega^{\rm bulk} \simeq 15.6\,$meV in GaAs) is replaced by $\Omega^{\rm MC}_{0\lambda}$ and the bulk photon wavevector p is replaced by $p_{\|}$. Note that for the MC 0λ-eigenmode the light field is homogeneous in the z-direction within the microcavity, i.e., for $|z| \leq L_z/2$. With increasing detuning from the X resonance the 1λ-LB and 0λ-LB polariton dispersions approach the photon frequencies $\omega^{\gamma}_{0\lambda} = cp_{\|}/\sqrt{\varepsilon_b}$ and $\tilde{\omega}^{\gamma}_{0\lambda} = cp_{\|}/\sqrt{\varepsilon^{(0)}_b}$, respectively, where the low-frequency dielectric constant is given by $\varepsilon^{(0)}_b = \varepsilon_b[1 + (\Omega^{\rm MC}_{0\lambda}/\omega_t)^2]$. The interconnection between two MC polariton domains occurs via the 1λ-LB polariton dispersion: With increasing $p_{\|}$ from $p_{\|} \lesssim p^{(1\lambda)}_{\|}$ towards $p_{\|} \gtrsim p_0$ the structure of the photon component of 1λ-LB polaritons smoothly changes, as a superposition of two modes, from purely 1λ-mode to purely 0λ-mode.

Because $1/a^{\rm (2D)}_{\rm XX} > p_0$, the non-zero exciton component of all three MC polariton dispersion branches contributes to the molecule state and, therefore, to the XX-mediated optics of microcavities. The X component, associated with the 0λ-LB, 1λ-LB, and 1λ-UB dispersions, is given by

$$(u^{\rm MC}_i)^2 = \left[1 \;+\; \frac{\omega_i^4(\Omega^{\rm MC}_{1\lambda})^2}{\omega_t\omega^{\gamma}_{1\lambda}[\omega_i^2 - (\omega^{\gamma}_{1\lambda})^2]^2} \right.$$
$$\left. +\; \frac{\omega_i^4(\Omega^{\rm MC}_{0\lambda})^2}{\omega_t\omega^{\gamma}_{0\lambda}[\omega_i^2 - (\omega^{\gamma}_{0\lambda})^2]^2}\right]^{-1}, \qquad (10)$$

where $\omega_{i=0\lambda{\rm LB},1\lambda{\rm LB},1\lambda{\rm UB}} = \omega^{\rm MC}_{i=0\lambda{\rm LB},1\lambda{\rm LB},1\lambda{\rm UB}}(p_{\|})$ are the polariton dispersion branches calculated with Eq. (6). For a given $p_{\|}$ the X components satisfy the sum rule, $(u^{\rm MC}_{0\lambda{\rm LB}})^2 + (u^{\rm MC}_{1\lambda{\rm LB}})^2 + (u^{\rm MC}_{1\lambda{\rm UB}})^2 = 1$. The exciton components, which correspond to the 0λ-LB, 1λ-LB, and 1λ-UB dispersions shown in Fig. 1, are plotted in Fig. 2. The above polariton branches have non-zero X component when the frequencies $\omega^{\rm MC}_i(p_{\|})$ resonate with the X state, i.e., at $p_{\|} \lesssim p^{(1\lambda)}_{\|}$ for the 1λ-UB, at $p_{\|} \lesssim p_0$ for the 1λ-LB, and at $p_{\|} \gtrsim p_0$ for the 0λ-LB, respectively (see Fig. 2). In our microcavities the X component of the 2λ-, 3λ- etc. eigenmode MC polaritons is negligible.

A non-ideal optical confinement of the MC photon modes by distributed Bragg reflectors (DBRs) leads to the leakage of MC photons and gives rise to the radiative rate $\gamma_{\rm R}$ in Eq. (6). Thus the radiative width of MC polaritons, due to their optical escape through the DBRs, is $\Gamma^{\rm MC}_{i=0\lambda{\rm LB},1\lambda{\rm LB},1\lambda{\rm UB}} = \hbar(v^{\rm MC}_{i=0\lambda{\rm LB},1\lambda{\rm LB},1\lambda{\rm UB}})^2\gamma_{\rm R}$,

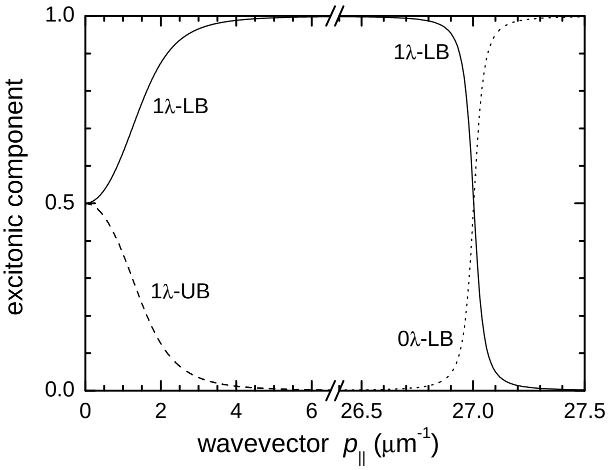

FIG. 2: The exciton component of 0λ-LB (dotted line), 1λ-LB (solid line), and 1λ-UB (dashed line) polaritons in a zero-detuning GaAs microcavity.

where the photon component of the polaritons is given by $(v_i^{\rm MC})^2 = 1 - (u_i^{\rm MC})^2$. Note that for our GaAs-based macrocavities at low temperatures, $\gamma_{\rm R}$ is much larger than $\gamma_{\rm X}$[26,27].

B. Bipolaritons in GaAs quantum wells

The quasi-2D excitonic molecules in single QWs without co-planar optical confinement of the light field can either resonantly dissociate into interface polaritons or decay radiatively into the bulk photon modes. In our optical experiments, which deal with pump and signal bulk photons only, the first route of the XX optical decay cannot be visualized directly. Thus this channel refers to the "hidden" optics associated with the evanescent light field resonantly guided by QW excitons.

(i) *Resonant dissociation of QW excitonic molecules into outgoing interface polaritons.* The bipolariton model allows us to calculate the XX radiative width $\Gamma_{\rm XX}^{\rm QW(1)} = \Gamma_{\rm XX}^{\rm QW(1)}(\mathbf{K}_{\|})$, associated with the resonant dissociation of the molecule with in-plane translational momentum $\hbar\mathbf{K}_{\|}$, by solving the wave equation[18,19]:

$$\Big[E_{\rm IP}(\mathbf{p}_{\|} + \mathbf{K}_{\|}/2) + E_{\rm IP}(-\mathbf{p}_{\|} + \mathbf{K}_{\|}/2)\Big]\tilde{\Psi}_{\rm XX}(\mathbf{p}_{\|}, \mathbf{K}_{\|}) + f_{\rm IP}(\mathbf{p}_{\|}, \mathbf{K}_{\|}) \sum_{\mathbf{p}'_{\|}} W_{\sigma^+\sigma^-}(\mathbf{p}_{\|} - \mathbf{p'}_{\|})\tilde{\Psi}_{\rm XX}(\mathbf{p'}_{\|}, \mathbf{K}_{\|}) = \tilde{E}_{\rm XX}^{\rm QW}(\mathbf{K}_{\|})\tilde{\Psi}_{\rm XX}(\mathbf{p}_{\|}, \mathbf{K}_{\|}) \,. \qquad (11)$$

Here $\tilde{\Psi}_{\rm XX}$ and $\tilde{E}_{\rm XX}^{\rm QW}$ are the bipolariton (XX) wavefunction and energy, respectively, $E_{\rm IP} = \hbar\omega_{\rm IP}$ is the QW polariton energy determined by the dispersion Eq. (1), $f_{\rm IP}(\mathbf{p}_{\|}, \mathbf{K}_{\|}) = u_{\rm IP}^2(\mathbf{p}_{\|} + \mathbf{K}_{\|}/2)u_{\rm IP}^2(-\mathbf{p}_{\|} + \mathbf{K}_{\|}/2)$, where $u_{\rm IP}^2$ is given by Eq. (2), $\hbar\mathbf{p}_{\|}$ is the in-plane momentum of the relative motion of the optically-dressed constituent excitons, and $W_{\sigma^+\sigma^-}$ is the attractive Coulombic potential between σ^+- and σ^-- polarized QW excitons. The complex bipolariton energy can also be rewritten as $\tilde{E}_{\rm XX}^{\rm QW} = 2E_{\rm X} - \epsilon_{\rm XX}^{(0)} + \Delta_{\rm XX}^{\rm QW} - i\Gamma_{\rm XX}^{\rm QW}/2$, where $\epsilon_{\rm XX}^{(0)}$ is the XX binding energy with no renormalization by the coupling with the vacuum light field. For the non-local deuteron model potential $W_{\sigma^+\sigma^-}(|\mathbf{p}_{\|} - \mathbf{p'}_{\|}|)$, which yields within the standard Schrödinger two-particle (two-X) equation the wavefunction $\Psi_{\rm XX}^{(0)}(p_{\|}) = 2\sqrt{2\pi}a_{\rm XX}^{\rm (2D)}/[(p_{\|}a_{\rm XX}^{\rm (2D)})^2 + 1]^{3/2}$ for an optically inactive molecule, the bipolariton wave Eq. (11) is exactly-solvable[18]. The input parameters of the model are the binding energy $\epsilon_{\rm XX}^{(0)}$ and the oscillator strength $R_{\rm X}^{\rm QW}$. Thus the exactly-solvable bipolariton model simplifies the exciton-exciton interaction, but treats rigorously the (interface) polariton effect.

(ii) *Resonant decay of QW excitonic molecules into the bulk photon modes.* The decay occurs when at least one of the constituent excitons of a QW molecule moves within the radiative zone, i.e., when $|+\mathbf{p}_{\|} + \mathbf{K}_{\|}/2| \leq p_0$ and/or $|-\mathbf{p}_{\|} + \mathbf{K}_{\|}/2| \leq p_0$. Note that the exciton-exciton resonant coherent Coulombic scattering within the molecule state intrinsically couples the X radiative and QW polariton modes. Thus the XX width, associated with the optical decay into the bulk photon modes, is given by

$$\Gamma_{\rm XX}^{\rm QW(2)}(\mathbf{K}_{\|}\!=\!0) = \frac{1}{\pi}\int_0^{p_0} |\Psi_{\rm XX}^{(0)}(2p_{\|})|^2 \Gamma_{\rm X}^{\rm QW}(p_{\|}) p_{\|} dp_{\|} = \hbar\frac{\sqrt{\varepsilon_b}}{c}R_{\rm X}^{\rm QW}\frac{\sqrt{\chi}}{4(1+\chi)^{5/2}}\Big[(5+2\chi)\sqrt{\chi(1+\chi)} + 3\ln(\sqrt{1+\chi} + \sqrt{\chi})\Big] \,, \qquad (12)$$

where $\chi = 4\delta_{\rm R}^{\rm (2D)} \equiv 4(a_{\rm XX}^{\rm (2D)}p_0)^2$ and $\Gamma_{\rm X}^{\rm QW}(p_{\|})$ is given by Eq. (3). In the above integral over the QW radiative zone we approximate $\Psi_{\rm XX}^{(0)}$ by the deuteron wavefunction. For $\chi \ll 1$ Eq. (12) yields $\Gamma_{\rm XX}^{\rm QW(2)} \simeq 2\hbar(\sqrt{\varepsilon_b}/c)\chi R_{\rm X}^{\rm QW} = 8(a_{\rm XX}^{\rm (2D)}p_0)^2\Gamma_{\rm X}^{\rm QW}(p_{\|}\!=\!0)$. However, for our reference GaAs QW with weak confinement of the electronic states one has $\chi \simeq 1.2$ so that the above simple approximation of Eq. (12) cannot be used.

In Fig. 3 we plot the radiative widths $\Gamma_{\rm X}^{\rm QW}(\mathbf{p}_{\|}\!=\!0)$, $\Gamma_{\rm XX}^{\rm QW(1)}(\mathbf{K}_{\|}\!=\!0)$, $\Gamma_{\rm XX}^{\rm QW(2)}(\mathbf{K}_{\|}\!=\!0)$, and $\Gamma_{\rm XX}^{\rm QW(1)}(\mathbf{K}_{\|}\!=\!0) + \Gamma_{\rm XX}^{\rm QW(2)}(\mathbf{K}_{\|}\!=\!0)$ against the oscillator strength of QW excitons $R_{\rm X}^{\rm QW}$. The widths are calculated with Eqs. (11) and (12) for the input XX binding energy $\epsilon_{\rm XX}^{(0)} = 1.1\,$meV. As we discuss in Section III, the oscillator strength $R_{\rm X}^{\rm QW}$ of the high-quality reference QW used in our experiments is given by $\hbar^2 R_{\rm X}^{\rm QW}(d_z\!=\!250\,\mathring{A}) \simeq 0.035\,{\rm eV}^2\mathring{A}$. The above value, which is inferred from the experimental data, refers to the GaAs QW sandwiched between semi-infinite bulk AlGaAs barriers and is consistent with that estimated in the previous Subsection by using Eq. (5). A cap layer on top of the reference single QW modifies the evanescent field associated with interface polaritons and reduces the oscillator strength to $\hbar^2 \tilde{R}_{\rm X}^{\rm QW}(d_z\!=\!250\,\mathring{A}) \simeq$

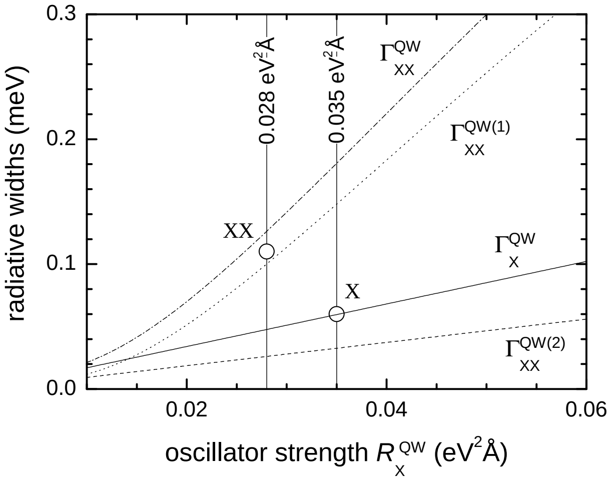

FIG. 3: The calculated radiative decay widths of the exciton and bipolariton states versus the oscillator strength R_X^{QW}. The XX radiative widths associated with the decay into interface polaritons, $\Gamma_{XX}^{QW(1)}$, and into bulk photon modes, $\Gamma_{XX}^{QW(2)}$, are plotted separately. The input XX binding energy $\epsilon_{XX}^{(0)} = 1.1\,$meV. The two circle symbols show Γ_X^{QW} and Γ_{XX}^{QW} inferred from the experimental data.

$0.028\,\text{eV}^2\mathring{A}$ (for the details see Section IV). As shown in Fig. 3, for $\hbar^2 R_X^{QW} = 0.035\,\text{eV}^2\mathring{A}$ Eqs. (11) and (12) yield $\Gamma_{XX}^{QW(1)}(\mathbf{K}_\|{=}0) \simeq 148\,\mu\text{eV}$ and $\Gamma_{XX}^{QW(2)}(\mathbf{K}_\|{=}0) \simeq 33\,\mu\text{eV}$, so that the total XX radiative width is given by $\Gamma_{XX}^{QW}(\mathbf{K}_\|{=}0) = \Gamma_{XX}^{QW(1)} + \Gamma_{XX}^{QW(2)} \simeq 0.18\,\text{meV}$. For $\hbar^2 \tilde{R}_X^{QW} \simeq 0.028\,\text{eV}^2\mathring{A}$ one calculates $\Gamma_{XX}^{QW(1)}(\mathbf{K}_\|{=}0) \simeq 100\,\mu\text{eV}$, $\Gamma_{XX}^{QW(2)}(\mathbf{K}_\|{=}0) \simeq 26\,\mu\text{eV}$, and $\Gamma_{XX}^{QW}(\mathbf{K}_\|{=}0) = \Gamma_{XX}^{QW(1)} + \Gamma_{XX}^{QW(2)} \simeq 0.126\,\text{meV}$. The latter value is indeed very close to the XX radiative width $\Gamma_{XX}^{QW} \simeq 0.1\,\text{meV}$ inferred from our opical experiments with the reference QW (see Section III).

The photon-assisted resonant dissociation of QW molecules into outgoing interface polaritons is more efficient than the XX optical decay into the bulk photon modes by factor 4.5 for $\hbar^2 R_X^{QW} \simeq 0.035\,\text{eV}^2\mathring{A}$ and by factor 3.8 for $\hbar^2 \tilde{R}_X^{QW} \simeq 0.028\,\text{eV}^2\mathring{A}$, respectively. This conclusion is consistent with that of Ref. [24], where for the limit of strong QW confinement ($d_z \rightarrow 0$) the relative efficiency of the two optical decay channels was estimated to be $\Gamma_{XX}^{QW(1)} : \Gamma_{XX}^{QW(2)} \simeq 25 : 1$. The latter ratio refers to the idealized case of an extremely narrow GaAs QW surrounded by infinitely thick AlGaAs barriers. The resonant optical dissociation of the QW molecules into interface polaritons is much stronger than the radiative decay into the bulk photon modes, because the constituent excitons in their relative motion move mainly outside the radiative zone, with the in-plane momenta $|\pm\mathbf{p}_\| + \mathbf{K}_\|/2| \gtrsim p_0$. In this case the excitons are optically dressed by the evanescent light field, i.e., they exist as QW polaritons and, therefore, decay mainly into the confined, QW-guided interface modes. The picture can also be justified by analyzing the joint density of states relevant to the two optical decay channels. Note that in both main equations, Eq. (11) and Eq. (12), $\delta_R^{(2D)} = (a_{XX}^{(2D)} p_0)^2$ does represent the dimensionless smallness parameter of the (bipolariton) model.

C. Bipolaritons in GaAs-based microcavities

The bipolariton model for excitonic molecules in λ-microcavities requires to construct the XX state in terms of quasi-bound 0λ-LB, 1λ-LB, and 1λ-UB polaritons. In this case the radiative corrections to the XX state with $\mathbf{K}_\| = 0$ are given by

$$\begin{aligned} \Delta_{XX}^{MC}(\mathbf{K}_\|{=}0) &= \frac{27}{8}\sqrt{\frac{\pi}{2}}\,\epsilon_{XX}^{(0)}\,\mathrm{Re}\Big\{\frac{A}{1+B}\Big\}, \\ \Gamma_{XX}^{MC}(\mathbf{K}_\|{=}0) &= -\frac{27}{4}\sqrt{\frac{\pi}{2}}\,\epsilon_{XX}^{(0)}\,\mathrm{Im}\Big\{\frac{A}{1+B}\Big\}, \end{aligned} \quad (13)$$

where

$$\begin{aligned} A &= \frac{1}{2\pi}\int_0^{+\infty} p_\| dp_\| \left[\tilde{G}(p_\|)\left(\epsilon_{XX}^{(0)} + \frac{\hbar^2 p_\|^2}{M_x}\right) + 1\right]\Psi_{XX}^{(0)}(p_\|), \\ B &= \frac{27}{16}\frac{1}{\sqrt{2\pi}}\,\epsilon_{XX}^{(0)}\int_0^{+\infty} p_\| dp_\|\,\tilde{G}(p_\|)\Psi_{XX}^{(0)}(p_\|). \end{aligned} \quad (14)$$

In Eq. (14) the bipolariton Green function $\tilde{G}(p_\|)$ is

$$\tilde{G}(p_\|) = \sum_{i,j}\frac{[u_i^{MC}(p_\|)u_j^{MC}(-p_\|)]^2}{E_{XX}^{MC} - \hbar\omega_i^{MC}(p_\|) - \hbar\omega_j^{MC}(-p_\|) + i\gamma_0}, \quad (15)$$

where $E_{XX}^{MC} = 2E_X(p_\|{=}0) - \epsilon_{XX}^{(0)}$, the MC polariton eigenfrequency $\omega_{i(j)}^{MC}$ and the X component $[u_{i(j)}^{MC}]^2$ with $i, j = 0\lambda$-LB, 1λ-LB, and 1λ-UB are given by Eq. (6) and Eq. (10), respectively, and $\gamma_0 \rightarrow +0$. The XX radiative corrections, i.e., the Lamb shift Δ_{XX}^{MC} and the radiative width Γ_{XX}^{MC}, depend upon the relative motion of the constituent QW excitons over whole momentum space, i.e., Eqs. (13)-(14) include integration over $dp_\|$. The change of the input XX binding energy, $\epsilon_{XX}^{(0)} \rightarrow \epsilon^{XX} = \epsilon_{XX}^{(0)} - \Delta_{XX}^{MC}(\mathbf{K}_\|) + (i/2)\Gamma_{XX}^{MC}(\mathbf{K}_\|)$, occurs because in their relative motion the constituent excitons move along the MC polariton dispersion curves, rather than possess the quadratic dispersion, $E_X = \hbar\omega_t + \hbar^2 p_\|^2/(2M_x)$ (the latter is valid only for optically inactive excitons).

The solution of the exactly-solvable bipolariton model, given by Eqs. (13)-(15), includes all possible channels of the in-plane dissociation of the microcavity molecule into two outgoing MC polaritons, i.e., "XX ($\mathbf{K}_\|{=}0$) → ith-branch MC polariton ($\sigma^+, \mathbf{p}_\|$) + jth-branch MC polariton ($\sigma^-, -\mathbf{p}_\|$)". Note that the solution of the bipolariton wave Eq. (11) for excitonic molecules in a single QW can be obtained from Eqs. (13)-(15) by putting $i = j =$ IP and replacing $u_{i(j)}^{MC}$ and $\omega_{i(j)}^{MC}$ by u_{IP} and ω_{IP}, respectively.

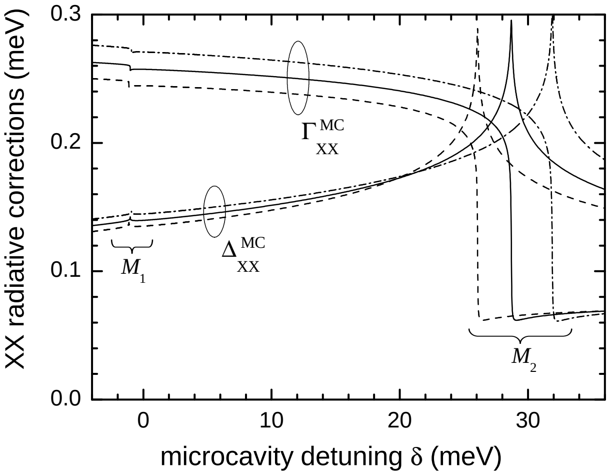

FIG. 4: The radiative corrections to the excitonic molecule state, $\Gamma_{\rm XX}^{\rm MC}$ and $\Delta_{\rm XX}^{\rm MC}$, calculated against the MC detuning δ with Eqs. (13)-(15) for the MC Rabi energies $\hbar\Omega_{1\lambda}^{\rm MC} = 7.76\,$meV and $\hbar\Omega_{0\lambda}^{\rm MC} = 5.60\,$meV. The input XX binding energy $\epsilon_{\rm XX}^{(0)}$ is 0.9 meV (dash-dotted line), 1.0 meV (solid line), and 1.1 meV (dashed line).

The radiative width $\Gamma_{\rm XX}^{\rm MC(1)} = \Gamma_{\rm XX}^{\rm MC}(\delta)$ and the Lamb shift $\Delta_{\rm XX}^{\rm MC} = \Delta_{\rm XX}^{\rm MC}(\delta)$ calculated by Eqs. (13)-(15) as a function of the MC detuning $\delta = \hbar(\omega_0 - \omega_t)$ between the 1λ cavity mode and QW exciton are plotted in Fig. 4 for three values of the input XX binding energy, $\epsilon_{\rm XX}^{(0)} = 0.9\,$meV, 1.0 meV, and 1.1 meV. By applying Eq. (9), we estimate for this plot the Rabi frequencies, $\Omega_{1\lambda}^{\rm MC}$ and $\Omega_{0\lambda}^{\rm MC}$, relevant to the used three-branch MC polariton dispersion given by Eq. (6). Namely, for $\hbar^2 R_{\rm X}^{\rm QW} = 0.035\,{\rm eV}^2 \mathring{A}$, associated with the reference QW, and $L_z = 2326\,\mathring{A}$, Eq. (9) yields $\hbar\Omega_{1\lambda}^{\rm MC} \simeq 7.76\,$meV and $\hbar\Omega_{0\lambda}^{\rm MC} \simeq 5.60\,$meV. As a result of non-ideal optical confinement in the z-direction by DBRs, our GaAs-based λ-microcavity (i) has a smaller value of $\Omega_{1\lambda}^{\rm MC}$, i.e., $\hbar\Omega_{1\lambda}^{\rm MC} \simeq 3.7\,$meV and (ii) with increasing $p_\parallel$ loses the strength of optical confinement for MC 1λ-mode photons of frequency $\omega^\gamma \simeq \omega_0$. The latter means that the MC photon radiative width $\gamma_{\rm R}$ is $p_\parallel$-dependent and smoothly increases with increasing $p_\parallel$. The DBR optical confinement is completely relaxed for $p_\parallel \sim p_0$ so that the dispersion Eq. (6) becomes inadequate, and the microcavity 0λ-LB polariton dispersion evolves towards the interface polariton dispersion, associated with the single QW and given by Eq. (1). Thus, in order to model the experimental data with Eqs. (13)-(15), we use $\hbar\Omega_{1\lambda}^{\rm MC} \simeq 3.70\,$meV and $\hbar\Omega_{0\lambda}^{\rm MC} \simeq 2.67\,$meV, and replace the 0λ-LB polariton dispersion by the interface, QW polariton dispersion with $\hbar^2 R_{\rm X}^{\rm QW} = 0.035\,{\rm eV}^2 \mathring{A}$. For this case the plot of $\Gamma_{\rm XX}^{\rm MC}$ and $\Delta_{\rm XX}^{\rm MC}$ against the detuning δ is shown in Fig. 10 (for details see Section IV).

There are two sharp spikes in the dependence $\Delta_{\rm XX}^{\rm MC} = \Delta_{\rm XX}^{\rm MC}(\delta)$ which are accompanied by the jump-like changes of the XX radiative width $\Gamma_{\rm XX}^{\rm MC} = \Gamma_{\rm XX}^{\rm MC}(\delta)$ (see Figs. 4 and 10). The above structure is due to van Hove critical points, M_1 and M_2, in the joint density of the polariton states (JDPS) relevant to the optical decay "MC excitonic molecule $\mathbf{K}_\parallel$=0 $\rightarrow$ MC polariton $\mathbf{p}_\parallel$ + MC polariton $-\mathbf{p}_\parallel$" (for the critical points we use the classification and notations proposed in Ref. [28]). The first critical point M_1 in energy-momentum space $\{\delta, \mathbf{p}_\parallel\}$ refers to a negative MC detuning δ_1 and deals with the condition ${\rm Re}\{\tilde{E}_{\rm XX}^{\rm MC}(\mathbf{K}_\parallel{=}0)\} = 2\hbar\omega_t - \epsilon_{\rm XX}^{(0)} + \Delta_{\rm XX}^{\rm MC} = \hbar\omega_{1\lambda{\rm LB}}^{\rm MC}(\mathbf{p}_\parallel{=}0) + \hbar\omega_{1\lambda{\rm UB}}^{\rm MC}(-\mathbf{p}_\parallel{=}0)$. This point is marginal for the optical decay "XX $\rightarrow$ 1λ-LB polariton + 1λ-UB polariton": For $\delta \leq \delta_1$ the above channel is allowed, while it is absent for $\delta > \delta_1$. The critical point M_2 occurs at a positive detuning δ_2, which corresponds to the condition ${\rm Re}\{\tilde{E}_{\rm XX}^{\rm MC}(\mathbf{K}_\parallel{=}0)\} = 2\hbar\omega_t - \epsilon_{\rm XX}^{(0)} + \Delta_{\rm XX}^{\rm MC} = \hbar\omega_{1\lambda{\rm LB}}^{\rm MC}(\mathbf{p}_\parallel{=}0) + \hbar\omega_{1\lambda{\rm LB}}^{\rm MC}(-\mathbf{p}_\parallel{=}0)$, and is the main marginal point in the JDPS for the XX optical dissociation into two outgoing 1λ-LB polaritons. Namely, for $\delta \leq \delta_2$ the molecule can decay into two 1λ-LB polaritons, while for $\delta > \delta_2$ the optical decay of MC molecules with zero in-plane wavevector $\mathbf{K}_\parallel$ into 1λ-LB polaritons is completely forbidden. With a very high accuracy of the order of $|\delta|/\omega_t \ll 1$, one finds from Eq. (6) that $\hbar\omega_{1\lambda{\rm UB}/1\lambda{\rm LB}}(p_\parallel{=}0) = \hbar\omega_t + (\delta/2) \pm (1/2)[\delta^2 + (\hbar\Omega_{1\lambda}^{\rm MC})^2]^{1/2}$. Thus from the energy-momentum conservation law we estimate the detunings $\delta_{1,2}$:

$$\text{Critical point } M_1: \quad \delta_1 = -\epsilon_{\rm XX}^{\rm MC}\,,$$
$$\text{Critical point } M_2: \quad \delta_2 = \frac{(\hbar\Omega_{1\lambda}^{\rm MC})^2 - (\epsilon_{\rm XX}^{\rm MC})^2}{2\epsilon_{\rm XX}^{\rm MC}}\,, \qquad (16)$$

where $\epsilon_{\rm XX}^{\rm MC} = \epsilon_{\rm XX}^{(0)} - \Delta_{\rm XX}^{\rm MC}$ is the true, "measured" binding energy of the bipolariton state $\mathbf{K}_\parallel$=0, i.e., of the optically dressed molecule.

In order to visualize the optical decay channels of MC excitonic molecules, in Figs. 5 and 6 we plot the graphic solution of the energy-momentum conservation law, $E_{\rm XX}^{\rm MC} - \hbar\omega_i^{\rm MC}(p_\parallel) - \hbar\omega_j^{\rm MC}(-p_\parallel) = 0$ ($i, j = 0\lambda$-LB, 1λ-LB, and 1λ-UB). The roots of the equation are the poles of the bipolariton Green function $\tilde{G}$ given by Eq. (15). Figure 5, which refers to the zero-detuning GaAs-based microcavity, clearly illustrates that apart from the decay path "XX $\rightarrow$ 1λ-LB polariton + 1λ-LB polariton" there are also the decay routes which involve the 1λ-LB and 0λ-LB microcavity polaritons with $p_\parallel \sim p_0$, i.e., "XX $\rightarrow$ 0λ-LB polariton + 0λ-LB polariton" and "XX $\rightarrow$ 1λ-LB polariton + 0λ-LB polariton". The graphic solution of energy-momentum conservation for the wavevector domain $p_\parallel \lesssim p_\parallel^{(1\lambda)}$ is shown in a magnified scale in Figs. 6a-6c for $\delta = \delta_1$, 0, and δ_2, respectively. The touching points at $p_\parallel = 0$ between the 1λ-upper and 1λ-lower (see Fig. 6a) and 1λ-lower and 1λ-lower (see Fig. 6c) dispersion branches correspond to the M_1 and M_2 critical points, respectively. The graphic solution of the energy-momentum conservation law is shown in Fig. 6d for the vicinity of $p_\parallel = p_0$. According to Eq. (6), the 1λ-LB and 0λ-LB polaritons with $p_\parallel \sim p_0$ practically do not depend upon the MC detuning δ, i.e.,

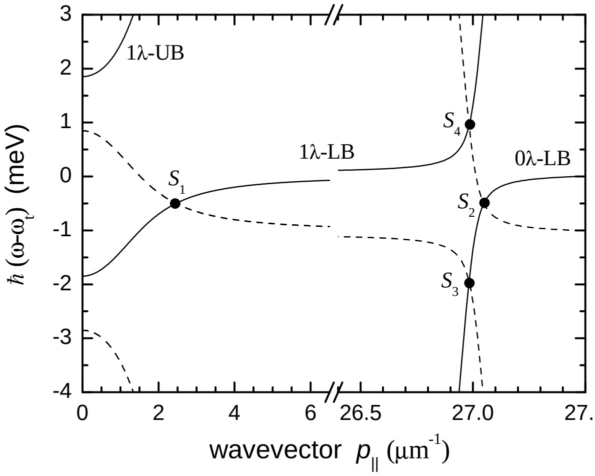

FIG. 5: The graphic solution of the energy-momentum conservation law for the optical decay of a MC molecule with $\mathbf{K}_\| = 0$. The microcavity Rabi energies are $\hbar\Omega^{\mathrm{MC}}_{1\lambda} = 3.70\,\mathrm{meV}$ and $\hbar\Omega^{\mathrm{MC}}_{0\lambda} = 2.67\,\mathrm{meV}$, the MC detuning is zero. The solutions are shown by the bold points S_1 (XX → 1λ-LB polariton + 1λ-LB polariton), S_2 (XX → 0λ-LB polariton + 0λ-LB polariton), and $S_{3,4}$ (XX → 0λ-LB polariton + 1λ-LB polariton). The efficiency of the last decay channel is negligible in comparison with that of the first two. The XX binding energy $\epsilon^{(0)}_{\mathrm{XX}} = 1\,\mathrm{meV}$.

the plot shown in Fig. 6d is not sensitive to δ.

The value of the $\Gamma^{\mathrm{MC}}_{\mathrm{XX}}$-jump and $\Delta^{\mathrm{MC}}_{\mathrm{XX}}$-spike nearby the critical point M_1, i.e., at $\delta = \delta_1$, shows that the contribution of the decay path "XX → 1λ-UB polariton + 1λ-LB polariton" is rather small, about 1-2% only. This is mainly due to a small value of the JDPS in the decay channel. The main contribution to the XX radiative corrections in microcavities is due to the frequency-degenerate decay routes "XX → 1λ-LB polariton + 1λ-LB polariton" and "XX → 0λ-LB polariton + 0λ-LB polariton" (or "XX → interface polariton + interface polariton", as a result of the relaxation of the transverse optical confinement at $p_\| \sim p_0$). The JDPS associated with the first main channel is given by

$$\rho^{\mathrm{XX}\to 1\lambda\mathrm{LB}+1\lambda\mathrm{LB}}_{\hbar\omega=\hbar\omega_t-\epsilon^{\mathrm{MC}}_{\mathrm{XX}}/2} = \frac{\pi}{2\hbar\omega_t}\left(a^{(2\mathrm{D})}_{\mathrm{XX}}p_0\right)^2 \times\left[1 + \left(\frac{\Omega^{\mathrm{MC}}_{1\lambda}}{\epsilon^{(0)}_{\mathrm{XX}}}\right)^2\right]\Theta(\delta_2-\delta)\,, \quad (17)$$

where $\Theta(x)$ is the Heaviside step function. The above JDPS is relevant to the calculations done by the bipolariton Eqs. (13)-(15). The appearance of the dimensionless parameter $\delta^{(2\mathrm{D})}_{\mathrm{R}} = (a^{(2\mathrm{D})}_{\mathrm{XX}}p_0)^2$ on the right-hand side (r.h.s.) of Eq. (17) is remarkable. Thus the same control parameter $\delta^{(2\mathrm{D})}_{\mathrm{R}}$ determines the optical decay of excitonic molecules in the reference single GaAs QW and in the GaAs-based microcavities. Furthermore, the JDPS given by Eq. (17) depends upon the MC detuning only through the step function $\Theta(\delta_2-\delta)$. The latter dependence gives rise to the critical point M_2. By comparing the XX radiative corrections for $\delta < \delta_2$ and $\delta > \delta_2$ (see Figs. 4 and 10), one concludes that the first main decay channel "XX → 1λ-LB polariton + 1λ-LB polariton" has nearly the same efficiency as the second one, "XX → 0λ-LB polariton + 0λ-LB polariton" (or "XX → interface polariton + interface polariton"). Note that the "virtual" decay paths, like "XX → 1λ-UB polariton + 1λ-UB polariton", still contribute to the XX Lamb shift in microcavities, according to Eqs. (13)-(15).

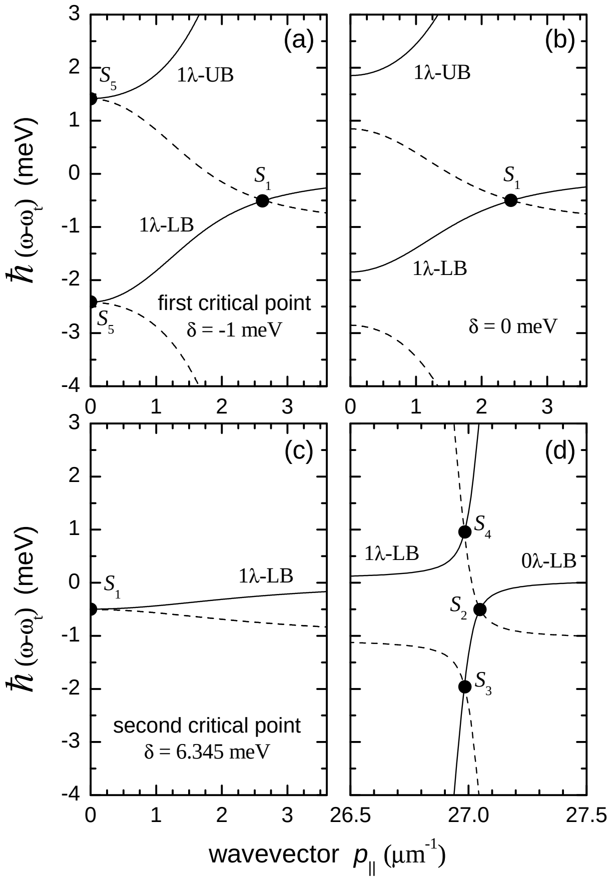

FIG. 6: The graphic solution of energy-momentum conservation for (a) the decay channels "XX → 1λ-LB polariton + 1λ-LB polariton" and "XX → 1λ-LB polariton + 1λ-UB polariton" (the MC detuning $\delta = -1\,\mathrm{meV}$, the marginal solution S_5 at $p_\| = 0$ refers to the critical point M_1); (b) the decay path "XX → 1λ-LB polariton + 1λ-LB polariton" (the MC detuning $\delta = 0$); (c) the decay path "XX → 1λ-LB polariton + 1λ-LB polariton" (the MC detuning $\delta = 6.345\,\mathrm{meV}$, the marginal solution S_1 at $p_\| = 0$ refers to the critical point M_2); (d) the decay channels "XX → 0λ-LB polariton + 0λ-LB polariton" and "XX → 0λ-LB polariton + 1λ-UB polariton" (this plot is practically independent of δ). The MC Rabi frequencies $\Omega^{\mathrm{MC}}_{1\lambda}$ and $\Omega^{\mathrm{MC}}_{0\lambda}$, and the XX binding energy $\epsilon^{(0)}_{\mathrm{XX}}$ are the same as in Fig. 5.

III. EXPERIMENT

The investigated sample consists of an MBE–grown GaAs/Al$_{0.3}$Ga$_{0.7}$As single quantum well of the thickness $d_z = 250\,\AA$ and placed in the center of a λ–cavity. An AlAs/Al$_{0.15}$Ga$_{0.85}$As DBR of 25 (16) periods was grown at the bottom (top) of the cavity. The spacer layer is wedged, in order to tune the cavity mode along the position on the sample. Details on the growth and sample design can be found in Ref. [11]. The optical properties of the reference single QW grown under nominally identical conditions are reported in Ref. [26]: The spectra show the ground-state heavy-hole (HH) and light-hole (LH) exciton absorption lines separated in energy by about 2.6 meV. In the MC sample, the coupling of both HH and LH excitons with the 1λ-mode cavity photons results in the formation of three 1λ-eigenmode MC polariton dispersion branches, 1λ-LB, 1λ-MB, and 1λ-UB[11]. The 1λ-mode polaritons have a narrow linewidth: The ratio between the HH Rabi splitting and the polariton linewidths at zero detuning is about twenty[27].

For the reference GaAs QW at temperature $T \lesssim 10\,\mathrm{K}$ the homogeneous width $\tilde{\Gamma}^{\mathrm{QW}}_{\mathrm{X}}$ is dominated by the radiative decay. The absorption linewidth, measured along the z-direction and extrapolated to zero temperature, yields the HH–X radiative width of $98 \pm 10\,\mu$eV. Note that this value is affected by optical interference which occurs at the position of the QW, $z = 0$, due to bulk photons emitted by the QW excitons and partly reflected back by the top surface ($z = L_{\mathrm{cap}} \simeq 499\,\mathrm{nm}$) of a cap layer. In this case one has a constructive interference which results in the enhancement of the light field at $z = 0$. By treating the optical interference effect, we estimate $\Gamma^{\mathrm{QW}}_{\mathrm{X}} \simeq 60\,\mu\mathrm{eV}$ for the reference QW sandwiched between semi-infinite bulk AlGaAs barriers. This radiative width yields the intrinsic oscillator strength of quasi-2D HH excitons $\hbar^2 R^{\mathrm{QW}}_{\mathrm{X}}(d_z{=}250\,\AA) \simeq 0.035\,\mathrm{eV}^2\AA$ (see Fig. 3). The measured characteristics of excitonic molecules in the reference QW are consistent with those reported in Ref. [26]: The XX binding energy $\epsilon^{\mathrm{MC}}_{\mathrm{XX}} \simeq 0.9 - 1.1\,\mathrm{meV}$ and the XX radiative width $\Gamma^{\mathrm{MC}}_{\mathrm{XX}} \simeq 0.1\,\mathrm{meV}$. The latter value is obtained by extrapolating the measured homogeneous width $\tilde{\Gamma}^{\mathrm{MC}}_{\mathrm{XX}} = \tilde{\Gamma}^{\mathrm{MC}}_{\mathrm{XX}}(T)$ to $T = 0\,\mathrm{K}$.

The optical experiments with the MC sample were performed using a Ti:sapphire laser source which generates Fourier-limited 100 fs laser pulses at 76 MHz repetition rate. Two exciting pulses, 1 and 2, with variable relative delay time τ_{12} propagate along two different incident directions $\mathbf{p}_{1,2}$ at small angle ($\leq 1°$) to the surface normal. Pulse 1 precedes pulse 2 for $\tau_{12} > 0$. The reflectivity spectra of the probe light and the FWM signal were analyzed with a spectrometer and a charge-coupled device camera of $140\,\mu$eV FWHM resolution. The sample was held in a Helium bath cryostat at T=5 K for all the pump-probe measurements and at T=9 K in the FWM experiments.

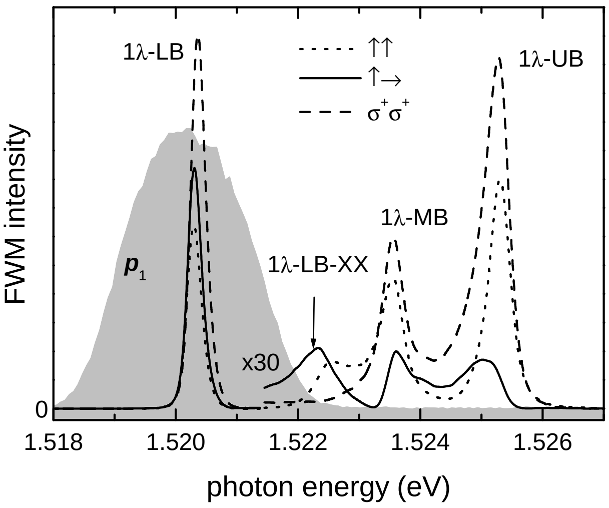

FIG. 7: Spectrally resolved four–wave mixing for co-circular (dashed line), co-linear (bold dotted line), and cross-linear (solid line) polarizations of the exciting pulses. The microcavity detuning is $\delta = 0.76\,\mathrm{meV}$. The pulse along $\mathbf{p}_1$-direction induces only 1λ-LB polaritons, and its spectrum is shown by the dotted line.

A. Bipolariton dephasing in GaAs microcavities

In order to measure the bipolariton dephasing we perform spectrally resolved FWM. The FWM signal was detected at $2\mathbf{p}_2 - \mathbf{p}_1$ in reflection geometry. The spot size of both exciting beams was $\sim 50\,\mu$m. In Fig. 7 we plot the spectrally–resolved FWM signal for different polarization configurations of the laser pulses. The positive detuning between the cavity 1λ-eigenmode and HH exciton is $\delta = 0.76\,\mathrm{meV}$, and the delay time is τ_{12}=1 ps. Pulse 1 of about 500 fs duration was spectrally shaped to *excite only the 1λ-LB polaritons*, and the FWM was probed with the spectrally broad pulse 2 at all 1λ-mode polariton resonances. For co–linear and cross-linear polarization configurations, the 1λ-LB polariton to excitonic molecule transition (1λ-LB – XX) is observed in the FWM signal (see arrow in Fig. 7) at a spectral position consistent with that found in our previous pump-probe experiments[10]. The XX-mediated FWM signal disappears for co–circular polarization, in accordance with the polarization selection rules for the two-photon generation of excitonic molecules in a GaAs QW.

Although the analysis of FWM in microcavities can be rather complicated[8,29], the interpretation of our measurements is simplified by the selective excitation of the 1λ-LB polaritons only. The observed TI–FWM is a free polarization decay, due to the dominant homogeneous broadening of the X lines in our high-quality $250\,\AA$-wide QWs[26]. At positive delays the FWM signal is created by the following sequence. At first, pulse 1 induces a first–order polarization associated with 1λ-LB polaritons. The induced polarization decays with the dephasing time $T^{1\lambda-\mathrm{LB}}_2$ of the 1λ-LB polaritons. The dephasing time

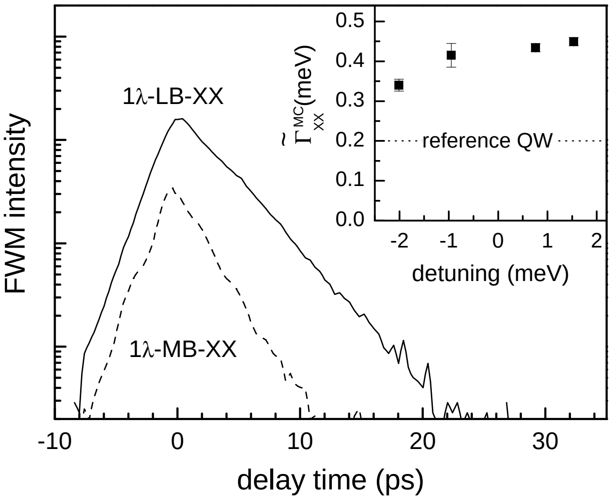

FIG. 8: Comparison between the FWM dynamics measured at the 1λ-LB – XX transition, when pulse 1 resonantly induces the 1λ-mode lower-branch polaritons only, and at the 1λ-MB – XX transition, when pulse 1 resonantly excites only the 1λ-mode middle-branch polaritons. Inset: The XX homogeneous linewidth $\tilde{\Gamma}_{XX}^{MC}$ against the MC detuning δ, measured at $T = 9\,K$ with about $4\,nJ/cm^2$ pump fluence.

$T_2^{1\lambda-LB}$ is dominated by the lifetime of 1λ-mode MC photons. Pulse 2 interacts nonlinearly with the induced polarization, and a third–order FWM signal is created with an amplitude that decreases with increasing τ_{12}, due to the decay of the first–order polarization associated with the 1λ-LB polaritons. The TI–FWM intensities at all probed resonances therefore decay nearly with the time constant $T_2^{1\lambda-LB}/2$. At negative τ_{12} the FWM signal stems from the two–photon coherence of the crystal ground state to the excitonic molecule transition (0–XX) induced by pulse 2. According to energy – in-plane momentum conservation, since pulse 1 is resonant with 1λ-LB polaritons only, the FWM signal, associated with bulk photons, is emitted in the direction $2\mathbf{p}_2-\mathbf{p}_1$ with the energy of the 1λ-LB – XX transition. Thus the TI–FWM dynamics at negative time delays allows us to study the polarization decay of the 0–XX transition[30], i.e., to find $\tilde{\Gamma}_{XX}^{MC}$.

The τ_{12}-dependence of the TI–FWM signals associated with the 1λ-LB – XX and 1λ-MB – XX transitions is shown in Fig. 8. As expected, at negative τ_{12} one finds the same dynamics for both transitions. Therefore, independently of the 1λ-eigenmode MC polariton branch selectively excited by pulse 1, we can infer the polarization decay rate of the 0–XX transition. The homogeneous linewidth of the 0–XX transition $\tilde{\Gamma}_{XX}^{MC}$ measured at low excitation energies per pulse ($\sim 4\,nJ/cm^2$) is potted against the MC detuning δ in the inset of Fig. 8. Only a weak detuning dependence of $\tilde{\Gamma}_{XX}^{MC}$ is observed for the detuning band $-2\,meV \le \delta \le 2\,meV$. Note that the deduced values $\tilde{\Gamma}_{XX}^{MC}(T{=}9\,K) \simeq 0.3 - 0.4\,meV$ are by factor $1.5 - 2$ larger than $\tilde{\Gamma}_{XX}^{QW} \simeq 0.2\,meV$ measured from the reference QW at nearly the same bath temperature T=10 K[26] (see the dotted line in the inset of Fig. 8).

B. The binding energy of bipolaritons in GaAs microcavities

The bipolariton energy E_{XX}^{MC} was found by analysing the pump-probe experiments. Pulse 1 acts as an intense pump while pulse 2 is a weak probe. The spectrum of the pump pulse is shaped and tuned in order to excite resonantly the 1λ-LB polaritons only. The spectrally broad probe pulse has a spot size of $\sim 40\,\mu m$. In this case the in-plane spatial gradient of the polariton energy is not significant. In order to achieve a uniform pump density over the probe area, the cross-section of the pump pulse is chosen to be by factor two larger than that of the probe light.

In Ref. [10] we show a well-resolved pump-induced absorption at the 1λ-LB – XX transition in the investigated MC sample. The 1λ-LB – XX absorption was observed in the reflectivity spectra at positive pump-probe delay times and for the cross-circularly (σ^+- and σ^--) polarized pump and probe pulses, according to the optical selection rules. In particularly, the induced absorption for three different positive MC detunings was measured. Here we extend the pump-probe experiment to study the detuning dependence $E_{XX}^{MC} = E_{XX}^{MC}(\delta)$, including $\delta < 0$. In Fig. 9 the probe reflectivity spectra measured at $\tau_{12} \simeq 0.5\,ps$ for the cross-circularly polarized pump and probe pulses is plotted. Indicated by the arrows (see Fig. 9), a spectrally well-resolved pump-induced absorption resonance is observed. In the upper left-hand side (l.h.s.) part of Fig. 9 the energy position of the 1λ-LB, 1λ-MB, and 1λ-UB polariton resonances and of the induced 1λ-LB – XX absorption are plotted against the MC detuning δ. The fit done with a three-coupled-oscillator scheme (1λ-eigenmode MC photon, HH exciton, and LH exciton resonances) are shown by the solid lines. The energies E_X^{HH} and E_X^{LH} of the HH and LH excitons ($E_X^{HH} \simeq 1.5219\,eV$ and $E_X^{LH} \simeq 1.5245\,eV$) are inferred from the fit, and the molecule energy E_{XX}^{MC} is determined as the sum of the measured 1λ-LB and 1λ-LB – XX transition energies. The bipolariton binding energy, evaluated as $\epsilon_{XX}^{MC} = 2E_X^{HH} - E_{XX}^{MC}$, is plotted against the MC detuning δ in the lower l.h.s. part of Fig. 9. We find that $\epsilon_{XX}^{MC} \simeq 0.9 - 1.1\,meV$, i.e., is similar to the value of ϵ_{XX}^{QW} in the reference single QW and slightly larger than that previously reported in Ref. [10].

IV. DISCUSSION

The optical decay of MC bipolaritons can also occur directly, through escape of the photon component of the constituent σ^+- and σ^--polarized MC polaritons into the bulk photon modes. The XX radiative width associated

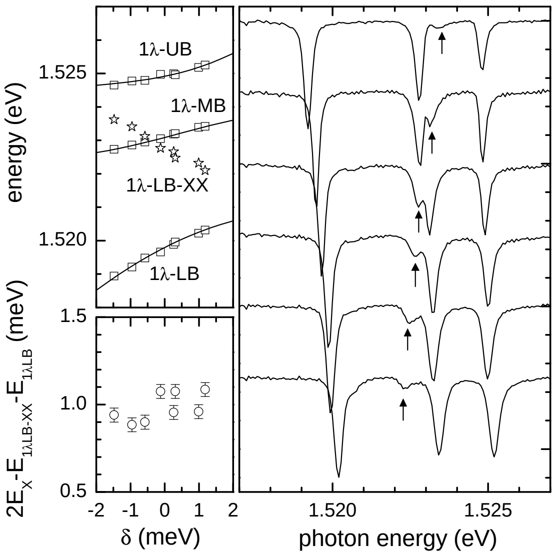

FIG. 9: The reflectivity spectra of the probe light at different detuning values. The spectra are measured for the cross-circularly polarized pump and probe pulses at delay time $\tau_{12} \simeq 0.5\,$ps and $T = 5\,$K. The pump fluence is about $0.1\,\mu$J/cm^2. The arrows indicate the 1λ-LP – XX pump-induced absorption. Upper left inset: The measured energy position of the 1λ-LP, 1λ-MP, 1λ-UP resonances (filled square points) and of the induced 1λ-LP – XX absorption (unfilled square points) versus the MC detuning δ. The fit of the MC polariton branches, associated with LH and HH QW excitons, is shown by the solid lines. Lower left inset: The XX binding energy $\epsilon^{\rm MC}_{\rm XX}$ determined as the difference between twice the bare HH exciton energy and the sum of the 1λ-LP and 1λ-LP – XX transition energies.

with this channel is given by

$$\Gamma^{\rm MC(2)}_{\rm XX}(\mathbf{K}_\parallel = 0) = \frac{\hbar}{\pi}\gamma_{\rm R}\int_0^\infty |\Psi^{(0)}_{\rm XX}(2p_\parallel)|^2 \times \Big[\sum_i \big[1-(u_i^{\rm MC})^2\big]\Big] p_\parallel dp_\parallel \,, \qquad (18)$$

where $u_i^{\rm MC} = u_i^{\rm MC}(p_\parallel)$ are determined by Eq. (10) and i runs over 0λ-LB, 1λ-LB, and 1λ-UB. Equation (18) is akin to Eq. (12) and can be interpreted in terms of optical evaporation of the MC excitonic molecules through the DBR mirrors. Using the measured radiative linewidth of 1λ-LB polaritons, $\Gamma^{\rm MC}_{\rm X}(p_\parallel \simeq 0.13\times 10^5\,{\rm cm}^{-1}) \simeq 0.1\,$meV, we estimate $\hbar\gamma_{\rm R} \simeq 0.3\,$meV, so that the radiative lifetime of MC photons is given by $\tau_{\rm R} \simeq 2.4\,$ps. In this case Eq. (18) yields $\Gamma^{\rm MC(2)}_{\rm XX} \simeq 1-2\,\mu$eV for $\epsilon^{(0)}_{\rm XX} \simeq 0.9-1.1\,$meV and assuming that $\gamma_{\rm R}$ is $p_\parallel$-independent. Thus $\Gamma^{\rm MC(2)}_{\rm XX}$ is less than $\Gamma^{\rm QW(2)}_{\rm XX}$, estimated with Eq. (12) for the reference QW (see Fig. 3), by more than one order of magnitude. This is because instead of the smallness parameter $\delta^{(2D)}_{\rm R} = (a^{(2D)}_{\rm XX} p_0)^2$, which appears on the r.h.s. of Eq. (12), Eq. (18) is scaled by $(a^{(2D)}_{\rm XX} p^{(1\lambda)}_\parallel)^2 \ll \delta^{(2D)}_{\rm R}$.

The radiative width $\Gamma^{\rm MC(2)}_{\rm XX}$, associated with the decay of XXs into the bulk photon modes, is by two orders of magnitude less than $\Gamma^{\rm MC(1)}_{\rm XX}$ calculated with Eqs. (13)-(15). Thus the resonant in-plane dissociation of molecules into outgoing MC polaritons absolutely dominates in the XX-mediated optics of microcavities, so that the total XX radiative width is given by $\Gamma^{\rm MC}_{\rm XX} = \Gamma^{\rm MC(1)}_{\rm XX} + \Gamma^{\rm MC(2)}_{\rm XX} \simeq \Gamma^{\rm MC(1)}_{\rm XX}$ (see Figs. 4 and 10). The extremely small value of $\Gamma^{\rm MC(2)}_{\rm XX}$ allows us to interpret a MC excitonic molecule as a nearly "optically-dark" state with respect to its direct decay into the bulk photon modes. However it is the resonant coupling between 1λ-mode cavity polaritons and external bulk photons which is responsible for the optical generation and probe of the XX states in microcavities: Our optical experiments deal only with bulk pump, probe, and signal photons. In the meantime the bipolariton wavefunction $\tilde{\Psi}_{\rm XX}$ is constructed in terms of 0λ-LB, 1λ-LB, and 1λ-UB polariton states, and umklapp between the MC polariton branches occurs through the coherent Coulombic scattering of two constituent polaritons.

While the interpretation of the experimental data (see Section III) does require three-branch, 1λ-LB, 1λ-MB, and 1λ-UB, polaritons associated with HH and LH excitons, the contribution to the XX optics from the LH Xs is very small. This occurs because (i) the energy $E^{\rm LH}_{\rm X}$ is well-separated from the XX-mediated resonance at $E^{\rm HH}_{\rm X} - \epsilon^{\rm MC}_{\rm XX}/2$ (the relevant ratio between $\epsilon^{\rm MC}_{\rm XX}/2$ and $E^{\rm LH}_{\rm X} - E^{\rm HH}_{\rm X} + \epsilon^{\rm MC}_{\rm XX}/2$ is equal to 0.16, i.e., is much less than unity) and (ii) because a contribution of the LH exciton to the total XX wavefunction is unfavorable in energy, i.e., is rather minor. We have checked numerically that by the first argument only the LH-X resonance cannot change the XX radiative corrections for more than 3-5%. Thus the bipolariton model we develop to analyze the optical properties of MC excitonic molecules and to explain the experimental data deals only with 0λ-LB, 1λ-LB, and 1λ-UB polaritons associated with the ground-state HH exciton.

In Fig. 10 we plot the XX radiative corrections against the MC detuning δ, calculated with Eqs. (13)-(15) by using the MC parameters adapted to our GaAs microcavities. Namely, the 1λ-mode cavity Rabi splitting is given by $\hbar\Omega^{\rm MC}_{1\lambda} = 3.7\,$meV, and we assume that the DBR optical confinement follows the step function $\Theta(p^{(1\lambda)}_\parallel - p_\parallel)$. For $p_\parallel \geq p^{(1\lambda)}_\parallel$ the 0λ-LB is replaced by the interface polariton dispersion given by Eq. (1). Due to the absence of the DBR transverse optical confinement at $p_\parallel \geq p^{(1\lambda)}_\parallel$, the resonant optical decay of the constituent excitons into the bulk photon mode is also included in our calculations by using Eq. (12) with integration over $dp_\parallel$ from $p^{(1\lambda)}_\parallel$ to p_0. From Fig. 10 we conclude that for the detuning band $-2\,{\rm meV} \lesssim \delta \lesssim 2\,$meV the radiative width $\Gamma^{\rm MC}_{\rm XX}$ is about $0.20 - 0.22\,$meV and indeed weakly depends upon δ, in accordance with our experimental data. A few μeV $\Gamma^{\rm MC}_{\rm XX}$-jump, associated with the critical point M_1, is too small to be detected in the current experi-

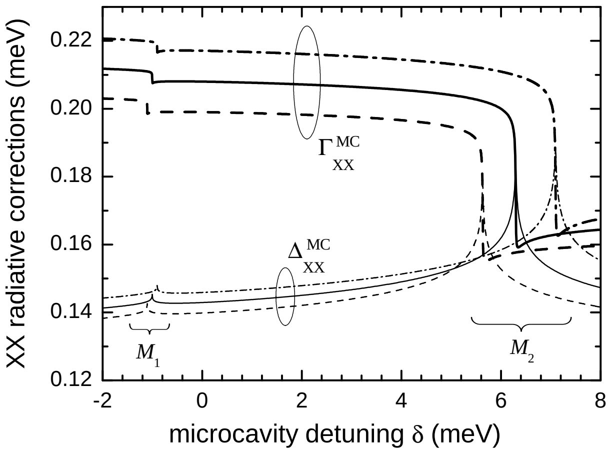

FIG. 10: The radiative corrections to the excitonic molecule state, $\Gamma^{\rm MC}_{\rm XX}$ and $\Delta^{\rm MC}_{\rm XX}$, calculated versus the MC detuning δ with Eqs. (13)-(15) for the MC Rabi energy $\hbar\Omega^{\rm MC}_{1\lambda} = 3.70\,$meV and assuming that the DBR optical confinement is completely relaxed for $p_\parallel \geq p_\parallel^{(1\lambda)} = 10^5\,{\rm cm}^{-1}$. In this case the 0$\lambda$-LB dispersion is replaced by the interface polariton dispersion with the oscillator strength $\hbar^2 R^{\rm QW}_{\rm X} = 0.035\,{\rm eV}^2\AA$. The input XX binding energy $\epsilon^{(0)}_{\rm XX}$ is 0.9 meV (dash-dotted line), 1.0 meV (solid line), and 1.1 meV (dashed line).

ments. Note that the contribution to $\Gamma^{\rm MC}_{\rm XX}$ from the decay channel "XX → 1λ-LB polariton + 1λ-LB polariton" can easily be estimated within a standard perturbation theory: $\Gamma^{\rm MC}_{\rm XX\to1\lambda LB+1\lambda LB} \simeq (\hbar\Omega^{\rm MC}_{1\lambda})^2 \rho^{\rm XX\to1\lambda LB+1\lambda LB}_{\hbar\omega=\hbar\omega_t-\epsilon^{\rm MC}_{\rm XX}/2}$, where the JDPS is given by Eq. (17). The above estimate yields $\Gamma^{\rm MC}_{\rm XX\to1\lambda LB+1\lambda LB} \simeq 0.06\,$meV and is consistent with the value of the $\Gamma^{\rm MC}_{\rm XX}$-jump around $\delta = \delta_2$, i.e., at the M_2 critical point (see Fig. 10). An observation of $\Gamma^{\rm MC}_{\rm XX} \simeq 0.10 - 0.15\,$meV at $\delta > \delta_2$, when the MC excitonic molecules become optically dark with respect to the decay into 1λ-mode MC polaritons, would be a direct visualization of the hidden decay path "XX → interface polariton + interface polariton".

The *relative* change of the XX radiative corrections is rather small to be observed in the tested MC detuning band $|\delta| \leq 2\,$meV with the current accuracy of our measurements: Eqs. (13)-(15) yield $\epsilon^{\rm MC}_{\rm XX}(\delta{=}2\,{\rm meV}) - \epsilon^{\rm MC}_{\rm XX}(\delta{=}-2\,{\rm meV}) \simeq -4\,\mu$eV and $\Gamma^{\rm MC}_{\rm XX}(\delta = 2\,{\rm meV}) - \Gamma^{\rm MC}_{\rm XX}(\delta = -2\,{\rm meV}) \simeq -5\,\mu$eV; the energy structure at $\delta = \delta_1 = -\epsilon^{\rm MC}_{\rm XX}$, i.e., nearby the critical point M_1, is also of a few μeV only (see Fig. 10). On the other hand, the GaAs-based microcavities we have now do not allow us to test the critical point M_2 which is located in the MC detuning band $5\,{\rm meV} < \delta < 8\,{\rm meV}$. In the latter case the relative change of $\Delta^{\rm MC}_{\rm XX}$ and $\Gamma^{\rm MC}_{\rm XX}$ is large enough, about $0.04 - 0.07\,$meV, to be detected in our experiments. High-precision modulation spectroscopy is very relevant to observation of the critical points, because the derivatives $\partial^n(\Delta^{\rm MC}_{\rm XX})/\partial\delta^n$ $(n \geq 1)$ and $\partial^n(\Gamma^{\rm MC}_{\rm XX})/\partial\delta^n$ $(n \geq 1)$ undergo a sharp change in the spectral vicinity of $M_{1,2}$. The modulation of δ can be done by applying time-dependent quasi-static electric[31], magnetic[32] or pressure[33] fields. Note that the measurement of the detunings δ_1 and δ_2 will allow us to determine with a very high accuracy, by using Eqs. (16), the XX binding energy $\epsilon^{\rm MC}_{\rm XX}$ and the MC Rabi frequency $\Omega^{\rm MC}_{1\lambda}$. A detailed study of the XX Lamb shift $\Delta^{\rm MC}_{\rm XX}$ versus the MC detuning δ and, in particular, the detection of the critical points M_1 and M_2 are the issue of our next experiments.

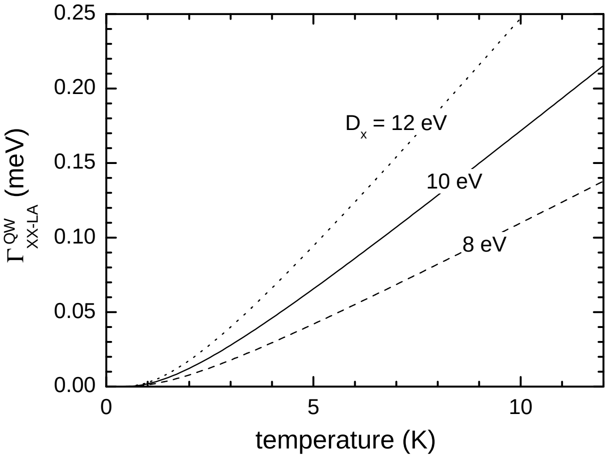

FIG. 11: The temperature dependence of the homogeneous width $\Gamma^{\rm QW}_{\rm XX-LA}$ associated with scattering of QW excitonic molecules by bulk LA-phonons. The calculations are done with Eq. (19) for the X deformation potential $D_x = 8\,$eV (dashed line), 10 eV (solid line), and 12 eV (dotted line).

In order to estimate the radiative width $\Gamma^{\rm MC}_{\rm XX}$ from the total homogeneous width $\tilde{\Gamma}^{\rm MC}_{\rm XX}$ measured at $T = 9\,$K in our FWM experiment, we assume that apart from the XX radiative decay the main contribution to $\tilde{\Gamma}^{\rm MC}_{\rm XX}$ is due to temperature-dependent XX – LA-phonon scattering. Note that in the experiment we deal with a low-intensity limit, when $\tilde{\Gamma}^{\rm MC}_{\rm XX}$ is nearly independent of the excitation level. Thus $\tilde{\Gamma}^{\rm MC}_{\rm XX} = \Gamma^{\rm MC}_{\rm XX} + \Gamma^{\rm QW}_{\rm XX-LA}$, where $\Gamma^{\rm QW}_{\rm XX-LA}$ is due to the scattering of QW molecules by bulk LA-phonons. The DBR optical confinement does not influence the XX – LA phonon scattering, so that the width $\Gamma^{\rm QW}_{\rm XX-LA} = \Gamma^{\rm QW}_{\rm XX-LA}(T)$ is the same for XXs in the reference single QW and in the microcavities. $\Gamma^{\rm QW}_{\rm XX-LA}$ is given by

$$\Gamma^{\rm QW}_{\rm XX-LA}(\mathbf{K}_\parallel{=}0) \;=\; 2\pi\frac{\hbar}{\tau_{\rm sc}}\int_1^\infty d\varepsilon\varepsilon\sqrt{\frac{\varepsilon}{\varepsilon-1}} \times\; |F_z(a\sqrt{\varepsilon(\varepsilon-1)})|^2 n^{\rm ph}_\varepsilon\,, \qquad (19)$$

where $\tau_{\rm sc} = (\pi^2\hbar^4\rho)/(32D_x^2M_x^3v_s)$, v_s is the longitudinal sound velocity, D_x is the X deformation potential, ρ is the crystal (GaAs) density, $n^{\rm ph}_\varepsilon = 1/[\exp(\varepsilon E_0/k_{\rm B}T) - 1]$, and $E_0 = 4M_xv_s^2$. The form-factor $F_z(x) = [\sin(x)/x][e^{ix}/(1{-}x^2/\pi^2)]$ refers to an infinite rectangular QW confinement potential and describes the relaxation of the momentum conservation law in the z-direction. The dimensionless parameter a is given by $a = (2d_zM_xv_s)/\hbar$.

The values of the deformation potential D_x, published in literature, disperse in the band $7\,\mathrm{eV} \leq D_x \leq 18\,\mathrm{eV}$. In Fig. 11 we plot $\Gamma^{\mathrm{QW}}_{\mathrm{XX-LA}} = \Gamma^{\mathrm{QW}}_{\mathrm{XX-LA}}(T)$ calculated by Eq. (19) for $D_x = 8$, 10, and $12\,\mathrm{eV}$. The deformation potential $D_x = 8\,\mathrm{eV}$, which gives $\Gamma^{\mathrm{QW}}_{\mathrm{XX-LA}}(T = 9\,\mathrm{K}) \simeq 0.094\,\mathrm{meV}$ and is close to $D_x \simeq 9.6\,\mathrm{eV}$ reported for GaAs in Ref. [34], fits the temperature dependence $\Gamma^{\mathrm{QW}}_{\mathrm{XX-LA}} = \Gamma^{\mathrm{QW}}_{\mathrm{XX-LA}}(T)$ measured for the reference QW. In particular, $\Gamma^{\mathrm{QW}}_{\mathrm{XX-LA}}(T = 10\,\mathrm{K}) \simeq 0.1\,\mathrm{meV}$ is inferred from the total $\tilde{\Gamma}^{\mathrm{QW}}_{\mathrm{XX}} \simeq 0.2\,\mathrm{meV}$ (see the inset of Fig. 8). Thus from our FWM measurements of $\tilde{\Gamma}^{\mathrm{MC}}_{\mathrm{XX}}$ at $T = 9\,\mathrm{K}$ we conclude that the XX radiative width $\Gamma^{\mathrm{MC}}_{\mathrm{XX}} = \tilde{\Gamma}^{\mathrm{MC}}_{\mathrm{XX}} - \Gamma^{\mathrm{QW}}_{\mathrm{XX-LA}}$ is about $0.2 - 0.3\,\mathrm{meV}$, i.e., is consistent with the values calculated within the bipolariton model (see Fig. 10).

In order to apply the bipolariton model [see Eq. (11)] to excitonic molecules in the reference single QW, one should take into account that the reference QW is sandwiched between a thick substrate and a cap layer of the thickness $L_{\mathrm{cap}} \simeq 499\,\mathrm{nm}$. The evanescent light field associated with the QW polaritons is modified by the cap layer. Indeed, for the $-\epsilon^{(0)}_{\mathrm{XX}}/2$ energy detuning from the X resonance, one estimates that $\kappa \simeq 1.4 \times 10^4\,\mathrm{cm}^{-1}$ so that $\exp(-\kappa L_{\mathrm{cap}}) \simeq 0.5$ is not negligible. The estimate refers to two frequency-degenerate outgoing interface polaritons ($\hbar\omega = E_{\mathrm{X}} - \epsilon^{(0)}_{\mathrm{XX}}0/2$) created in the photon-assisted resonant dissociation of the QW molecule with $\mathbf{K}_{\|} = 0$. At $z = L_{\mathrm{cap}}$ the initial evanescent field splits into two evanescent fields, "transmitted" to air (or vacuum) and "reflected" back towards the QW. The first light field very effectively decays in the z-direction, with $\kappa_{\mathrm{air}} = \sqrt{p_{\|}^2 - (\omega/c)^2} \simeq 2.6 \times 10^5\,\mathrm{cm}^{-1} \gg \kappa$. The "reflected" evanecsent light field makes at z=0 a destructive superposition with the initial evanecsent field, because the reflection coefficient of the top surface of the cap layer is $r_{\mathrm{cap}} = (\kappa - \kappa_{\mathrm{air}})/(\kappa + \kappa_{\mathrm{air}}) \simeq -0.9$. The destructive superposition stems from the π-jump of the phase of the "reflected" evanescsent field. Thus the effective oscillator strength relevant to the QW bipolariton wave Eq. (11) is given by $\tilde{R}^{\mathrm{QW}}_{\mathrm{X}} = R^{\mathrm{QW}}_{\mathrm{X}}[1 + (r_{\mathrm{cap}}/2)\exp(-2\kappa L_{\mathrm{cap}})]^2$. For our reference structure with $\hbar^2 R^{\mathrm{QW}}_{\mathrm{X}} \simeq 0.035\,\mathrm{eV}^2\mathring{A}$ we estimate $\hbar^2 \tilde{R}^{\mathrm{QW}}_{\mathrm{X}} \simeq 0.028\,\mathrm{eV}^2\mathring{A}$. In this case Eqs. (11)-(12) yield the total radiative width $\Gamma^{\mathrm{QW}}_{\mathrm{XX}}(\mathbf{K}_{\|}{=}0) \simeq 0.126\,\mathrm{meV}$ (see Fig. 3), the value which is very close to $\Gamma^{\mathrm{QW}}_{\mathrm{XX}} \simeq 0.1\,\mathrm{meV}$ obtained from the experimental data.

Thus the bipolariton model, which attributes the XX radiative corrections mainly to the in-plane dissociation of molecules into outgoing interface/MC polaritons, reproduce quantitatively the XX radiative widths $\Gamma^{\mathrm{MC}}_{\mathrm{XX}}$ and $\Gamma^{\mathrm{QW}}_{\mathrm{XX}}$ estimated from the experimental data. The two main channels for the XX decay in microcavities, "XX → 1λ-LB polariton + 1λ-LB polariton" and "XX → 0λ-LB (or interface) polariton + 0λ-LB (or interface) polariton" in comparison with the one leading decay route in single QWs, "XX → interface polariton + interface polariton", explain qualitatively the factor two difference between $\Gamma^{\mathrm{MC}}_{\mathrm{XX}}$ and $\Gamma^{\mathrm{QW}}_{\mathrm{XX}}$. The XX-mediated optics of microcavities does require to include the "hidden" 0λ-cavity (or interface, if the transverse optical confinement is relaxated for large $\mathbf{p}_{\|}$) polariton mode, which is invisible in standard optical experiments and, therefore, is usually neglected. Furthermore, with decreasing temperature $T \lesssim 10\,\mathrm{K}$ $\tilde{\Gamma}^{\mathrm{MC}}_{\mathrm{XX}}$ and $\tilde{\Gamma}^{\mathrm{QW}}_{\mathrm{XX}}$ effectively approach $\Gamma^{\mathrm{MC}}_{\mathrm{XX}}$ and $\Gamma^{\mathrm{QW}}_{\mathrm{XX}}$, respectively, so that the dephasing of the two-photon XX polarization in the microcavities and the reference QW occurs mainly through the optical decay of the molecules. Thus the $T_2 = 2T_1$ limit holds for the XX-mediated optics in our high-quality nanostructures and justifies the bipolariton model. The latter interprets the XX optical response in terms of resonant polariton-polariton scattering and requires nonperturbative treatment of both leading interactions, exciton-exciton Coulombic attraction and exciton-photon resonant coupling. Note that in our calculations with the exactly solvable bipolariton model only two control parameters of the theory, the input XX binding energy $\epsilon^{(0)}_{\mathrm{XX}}$ and the MC Rabi frequency $\Omega^{\mathrm{MC}}_{1\lambda}$ (or the X oscillator strength $R^{\mathrm{QW}}_{\mathrm{X}}$ for the reference QW), are taken from the experimental data. No fitting parameters are used in the numerical simulations.

The relative motion of two optically-dressed constituent excitons of the bipolariton eigenstate (i.e., of the excitonic molecule) is affected by the exciton-photon interaction, according to the polariton dispersion law. The optically-induced change of the X energy occurs not only in the close vicinity of the resonant crossover between the initial photon and exciton dispersions, but in a rather broad band of $\mathbf{p}$ (or $\mathbf{p}_{\|}$). For example, in bulk semiconductors the effective mass associated with the upper polariton dispersion branch at $p = 0$ is given by

$$M^{(3\mathrm{D})}_{\mathrm{UB}} \simeq \frac{M_x}{1 + 2(\omega_{\ell t}/\omega_t)[(M_x c^2/\varepsilon_b)/(\hbar\omega_t)]}\,. \qquad (20)$$

For bulk GaAs Eq. (20) yields $M_{\mathrm{eff}} = M^{(3\mathrm{D})}_{\mathrm{UB}}$ nearly by factor four less than the translational mass relevant to the pure excitonic dispersion, $M_x \simeq 0.7\,m_0$. From the microcavity dispersion Eq. (6) one estimates for $p_{\|} \to 0$ the effective masses associated with the 1λ-eigenmode polariton dispersion branches:

$$M^{(\mathrm{MC})}_{1\lambda\mathrm{UB/LB}}(\delta) \simeq \frac{2E_{\mathrm{X}}}{(c^2/\varepsilon_b)[1 \pm \delta/(\hbar\Omega^{\mathrm{MC}}_{1\lambda})]}\,, \qquad (21)$$

where we assume that $|\delta| \lesssim \hbar\Omega^{\mathrm{MC}}_{1\lambda}$. In particular, for a zero-detuning GaAs-based microcavity Eq. (21) yields $M^{(\mathrm{MC})}_{1\lambda\mathrm{UB}}(\delta{=}0) = M^{(\mathrm{MC})}_{1\lambda\mathrm{LB}}(\delta{=}0) = 2E_{\mathrm{X}}/(c^2/\varepsilon_b) \simeq 0.7 \times 10^{-4}\,m_0$. In the meantime, at relatively large in-plane momenta $p_{\|} \sim p^{(1\lambda)}_{\|} < p_0$ the 1λ-LB polariton energy smoothly approaches the exciton dispersion, i.e., $[E_{\mathrm{X}}(p_{\|}) - \hbar\omega^{\mathrm{MC}}_{1\lambda\mathrm{LB}}(p_{\|})]\big|_{p_{\|} \sim p^{(1\lambda)}_{\|}} \to [\hbar(\Omega^{\mathrm{MC}}_{1\lambda})^2\omega_t]/[2(c^2 p_{\|}^2/\varepsilon_b)] \propto 1/p_{\|}^2$, according to Eq. (6). While the above difference is rather small in absolute energy units, being compared with the in-plane kinetic energy of the exciton, $E^{\mathrm{X}}_{\mathrm{kin}} = \hbar^2 p_{\|}^2/2M_x$, it cannot be neglected. For example, the difference $E_{\rm X} - \hbar\omega^{\rm MC}_{1\lambda{\rm LB}}$ becomes equal to $E^{\rm X}_{\rm kin}$ at $p_{\|} \simeq 1.35 \times 10^5\,{\rm cm}^{-1}$. Note that for the above value of the in-plane wavevector $p_{\|}$ the photon component, associated with 1λ-LB polaritons, is negligible, i.e., $(u^{\rm MC}_{1\lambda{\rm LB}})^2 \simeq 1 \gg (v^{\rm MC}_{1\lambda{\rm LB}})^2$. Because it is a balance between the positive kinetic and negative interaction energies of the constituent excitons that gives rise to an excitonic molecule, the described optically-induced changes of the X effective mass at $p_{\|} = 0$ and the nonparabolicity of the X dispersion at large $p_{\|}$ are responsible for the large XX radiative corrections in quasi-2D GaAs nanostructures.

V. CONCLUSIONS

In this paper we have studied, both theoretically and experimentally, the optical properties of QW excitonic molecules in semiconductor (GaAs) microcavities. We attribute the main channel of the XX optical decay to the resonant dissociation of MC molecules into outgoing MC polaritons, so that the XX-mediated optical signal we detect is due to the resonant radiative escape of the secondary MC polaritons through the DBRs. The bipolariton model has been adapted to construct the XX wavefunction $\tilde{\Psi}_{\rm XX}$ in terms of two (1λ-UB, 1λ-LB and 0λ-LB) MC polaritons quasi-bound via Coulombic attraction of their exciton components. The MC bipolariton wave equation gives the radiative corrections to the XX state in microcavities. The following conclusions summarize our results.

(i) The radiative corrections to the excitonic molecule state in GaAs-based microcavities, the XX Lamb shift $\Delta^{\rm MC}_{\rm XX}$ and the XX radiative width $\Gamma^{\rm MC}_{\rm XX}$, are large (about $0.15 - 0.30$ of the XX binding energy $\epsilon^{(0)}_{\rm XX}$) and definitely cannot be neglected.

(ii) While usually the QW exciton – mediated optics of semiconductor microcavities is formulated in terms of two 1λ-mode polariton dispersion branches only (1λ-UB and 1λ-LB, according to the terminology used in our paper), we emphasize the importance of the 0λ-mode lower-branch polariton dispersion: The Coulombic interaction of the constituent excitons, which is responsible for the XX state, does couple intrinsically three relevant MC polariton branches, (1λ-UB, 1λ-LB, and 0λ-LB). Furthermore, the XX decay path "XX → 0λ-LB polariton + 0λ-LB polariton" is comparable in efficiency with the optical decay into 1λ-LB polariton modes, i.e., "XX → 1λ-LB polariton + 1λ-LB polariton". Due do the relaxation of the DBR optical confinement for in-plane wavevectors $p_{\|} \sim p_0 = \omega_t\sqrt{\varepsilon_b}/c$, with increasing $p_{\|}$ the 0λ-LB evolves towards the interface polariton dispersion associated with QW excitons. However, the short-wavelength LB polaritons with $p_{\|} \sim p_0$ always contribute to the XX-mediated optics of microcavities.

(iii) The zero-temperature extrapolation of the experimentally found XX dephasing width $\tilde{\Gamma}^{\rm MC}_{\rm XX}(T{=}9\,{\rm K})$ yields $\Gamma^{\rm MC}_{\rm XX}(T{=}0\,{\rm K}) \simeq 0.2 - 0.3\,{\rm meV}$ and is in a quantitative agreement with the result of the exactly solvable bipolariton model, $\Gamma^{\rm MC}_{\rm XX} \simeq 0.20 - 0.22\,{\rm meV}$. From the analysis of the experimental data we conclude that the bipolariton model of MC excitonic molecules, which requires $T_2 \simeq 2T_1$ limit, is valid for our high-quality GaAs-based nanostructures at $T \lesssim 10\,{\rm K}$. For the reference GaAs QW without the DBR transverse optical confinement we find $\Gamma^{\rm QW}_{\rm XX} = \tilde{\Gamma}^{\rm QW}_{\rm XX}(T{=}0\,{\rm K}) \simeq 0.1\,{\rm meV}$. The latter value is also quantitatively consistent with that calculated by solving the QW bipolariton wave equation, $\Gamma^{\rm QW}_{\rm XX} = 0.126\,{\rm meV}$. The nearly factor two difference between $\Gamma^{\rm QW}_{\rm XX}$ and $\Gamma^{\rm MC}_{\rm XX}$ clearly demonstrates the existence of the additional decay channel for a quasi-2D excitonic molecule in microcavities ["XX → interface polariton + interface polariton" in MC-free single QWs versus "XX → 0λ-LB (or interface) polariton + 0λ-LB (or interface) polariton" and "XX → 1λ-LB polariton + 1λ-LB polariton" for MC-embedded QW molecules].

(iv) The critical van Hove points, $M_1(\delta = \delta_1)$ and $M_2(\delta = \delta_2)$, in the JDPS of the resonant optical channel "XX ($\mathbf{K}_{\|}{=}0$) ↔ two 1λ-mode MC polaritons" can allow us to find accurately the molecule binding energy $\epsilon^{\rm MC}_{\rm XX}$ and the MC Rabi frequency $\Omega^{\rm MC}_{1\lambda}$. Thus, by using time-dependent MC detuning $\delta = \delta(t)$, we propose to develop high-precision modulation spectroscopies in order to detect the rapid changes of the XX radiative corrections at $\delta = \delta_{1,2}$ [spikes in the XX Lamb shift $\Delta^{\rm MC}_{\rm XX} = \Delta^{\rm MC}_{\rm XX}(\delta = \delta_{1,2})$ and jumps in the XX radiatve width $\Gamma^{\rm MC}_{\rm XX} = \Gamma^{\rm MC}_{\rm XX}(\delta = \delta_{1,2})$] and estimate $\epsilon^{\rm MC}_{\rm XX}$ and $\Omega^{\rm MC}_{1\lambda}$.

VI. ACKNOWLEDGMENTS

We appreciate valuable discussions with J. R. Jensen and J. M. Hvam. Support of this work by the DFG, EPSRC and EU RTN Project HPRN-CT-2002-00298 is gratefully acknowledged.

---

[1] V. M. Agranovich and O. A. Dubovskii, Pis'ma Zh. Teor. Fiz. **3**, 345 (1966) [JETP Lett. **3**, 223 (1966)].

[2] M. Nakayama, Solid State Commun. **55**, 1053 (1985).

[3] L. C. Andreani and F. Bassani, Phys. Rev. B **41**, 7536 (1990).

[4] C. Weisbuch, M. Nishioka, A. Ishikawa, and Y. Arakawa, Phys. Rev. Lett. **69**, 3314 (1992).

[5] V. Savona, Z. Hradil, A. Quattropani, and P. Schwendimann, Phys. Rev. B **49**, 8774 (1994).

[6] M. S. Skolnick, T. A. Fisher, and D. M. Whittaker, Semicond. Sci. Technol. **13**, 645 (1998).

[7] G. Khitrova, H. M. Gibbs, F. Jahnke, M. Kira, and S. W. Koch, Rev. Mod. Phys. **71**, 1591 (1999).

[8] M. Kuwata-Gonokami, S. Inouye, H. Suzuura, M. Shirane,

R. Shimano, T. Someya, and H. Sakaki, Phys. Rev. Lett. **79**, 1341 (1997).

[9] X. Fan, H. Wang, H. Q. Hou, and B. E. Hammons, Phys. Rev. B **57**, R9451 (1998).

[10] P. Borri, W. Langbein, U. Woggon, J. R. Jensen, and J. M. Hvam, Phys. Rev. B **62**, R7763 (2000).

[11] J. R. Jensen, P. Borri, W. Langbein, and J. M. Hvam, Appl. Phys. Lett. **76**, 3262 (2000).

[12] M. Saba, F. Quochi, C. Ciuti, U. Oesterle, J. L. Staehli, B. Deveaud, G. Bongiovanni, and A. Mura, Phys. Rev. Lett. **85**, 385 (2000).

[13] T. Baars, G. Dasbach, M. Bayer, and A. Forchel, Phys. Rev. B **63**, 165311 (2001).

[14] A. I. Tartakovskii, D. B. Krizhanovskii, D. A. Kurysh, V. D. Kulakovskii, M. S. Skolnick, and J. S. Roberts, phys. stat. sol. (a) **190**, 321 (2002).

[15] U. Neukirch, S. R. Bolton, N. A. Fromer, L. J. Sham, and D. S. Chemla, Phys. Rev. Lett. **84**, 2215 (2000).

[16] G. C. La Rocca, F. Bassani, and V. M. Agranovich, J. Opt. Soc. Am. B **15**, 652 (1998).

[17] C. Sieh, T. Meier, A. Knorr, F. Jahnke, P. Thomas, and S. W. Koch, Eur. Phys. J. B **11**, 407 (1999).

[18] A. L. Ivanov and H. Haug, Phys. Rev. Lett. **74**, 438 (1995).

[19] A. L. Ivanov, H. Haug, and L. V. Keldysh, Phys. Reports **296**, 237 (1998).

[20] D. S. Chemla, A. Maruani, and E. Batifol, Phys. Rev. Lett. **42**, 1075 (1979).

[21] H. Akiyama, T. Kuga, M. Matsuoka, and M. Kuwata-Gonokami, Phys. Rev. B **42**, 5621 (1990).

[22] E. Tokunaga, A. L. Ivanov, S. V. Nair, and Y. Masumoto, Phys. Rev. B **59**, R7837 (1999) and **63**, 233203 (2001).

[23] Ch. Mann, W. Langbein, U. Woggon, and A. L. Ivanov, Phys. Rev. B **64**, 235206 (2001).

[24] A. L. Ivanov, H. Wang, J. Shah, T. C. Damen, H. Haug, L. N. Pfeiffer, and L. V. Keldysh, Phys. Rev. B **56**, 3941 (1997).

[25] C. Weisbuch and R. G. Ulbrich, in *Light Scattering in Solids III*, Vol. 51 of *Topics in Applied Physics*, M. Cardona and G. Güntherodt (Eds.), Springer, Berlin 1982, p. 218.

[26] W. Langbein and J. M. Hvam, Phys. Rev. B **61**, 1692 (2000).

[27] P. Borri, J. R. Jensen, W. Langbein, and J. M. Hvam, Phys. Rev. B **61**, R13377 (2000).

[28] L. Van Hove, Phys. Rev. **89**, 1189 (1953).

[29] M. Shirane, C. Ramkumar, Y. P. Svirko, H. Suzuura, S. Inouye, R. Shimano, T. Someya, H. Sakaki, and M. Kuwata-Gonokami, Phys. Rev. B **58**, 7978 (1998).

[30] P. Borri, W. Langbein, U. Woggon, J. R. Jensen, and J. M. Hvam, phys. stat. sol. (a) **190**, 383 (2002).

[31] T. A. Fisher, A. M. Afshar, D. M. Whittaker, M. S. Skolnick, J. S. Roberts, G. Hill, and M. A. Pate, Phys. Rev. B **51**, 2600 (1995).

[32] A. Armitage, T. A. Fisher, M. S. Skolnick, D. M. Whittaker, P. Kinsler, and J. S. Roberts, Phys. Rev. B **55**, 16395 (1997).

[33] J. Zhang, H. Zhang, J. Chen, Y. Deng, Ch. Hu, L. An, F. Yang, G.-H. Li, and H. Zheng, J. Phys.: Condens. Matter **14**, 5349 (2002).

[34] F. H. Pollak and M. Cardona, Phys. Rev. **172**, 816 (1968).